

# Time Reversal Violation in Light Nuclei

A. Gnech<sup>a,b</sup>, M. Viviani<sup>b</sup>

<sup>a</sup>*Gran Sasso Science Institute, 67100 L'Aquila, Italy*

<sup>b</sup>*INFN-Pisa, 56127 Pisa, Italy*

(Dated: June 24, 2019)

Time Reversal Violation (TRV) interactions between quarks which appear in Standard Model (SM) and beyond-SM theories can induce TRV components in the nucleon-nucleon potential. The effects of these components can be studied by measuring the electric dipole moment (EDM) of light nuclei. In this work we present a complete derivation of the TRV nucleon-nucleon and three-nucleon potential up to next-to-next-to leading order (N<sup>2</sup>LO) in a chiral effective field theory ( $\chi$ EFT) framework. The TRV interaction is then used to evaluate the EDM of  $^2\text{H}$ ,  $^3\text{H}$  and  $^3\text{He}$  focusing in particular on the effects of the TRV three-body force and on the calculation of the theoretical errors. In case of a measurement of the EDM of these nuclei, the result of present work would permit to determine the values of the low energy constants and to identify the source of TRV.

## I. INTRODUCTION

The violation of parity (P) with the conservation of charge conjugation (C) generates a CP violation that, using the CPT theorem, results in a time reversal violation (TRV). TRV is a key ingredient in the explanation of the observed matter-antimatter asymmetry in the Universe [1]. The Standard Model (SM) has a natural source of CP-violation in the Cabibbo-Kobayashi-Maskawa (CKM) quark mixing matrix, however this mechanism is not sufficient for explaining the observed asymmetry [2]. This discrepancy opens a window in possible TRV effect in the SM, such as the  $\theta$ -term in the Quantum Chromodynamics (QCD) sector [3], or in other sources of beyond-SM (BSM) theories [4].

The measurement of Electric Dipole Moments (EDMs) of particles is the most promising observable for studying TRV beyond CKM mixing matrix effects. Indeed, the EDM induced by the complex phase of the CKM matrix are suppressed since the EDM does not involve flavour changing [4–7]. Therefore, any non-vanishing EDM of a nuclear or an atomic system would highlight TRV effects beyond the CKM mixing matrix. The present experimental upper bounds on the EDMs of neutron and proton are  $|d_n| < 2.9 \cdot 10^{-13} e \text{ fm}$  [8] and  $|d_p| < 7.9 \cdot 10^{-12} e \text{ fm}$ , where the proton EDM has been inferred from a measurement of the diamagnetic  $^{199}\text{Hg}$  atom [9] using a calculation of the nuclear Schiff moment [10]. For the electron, the most recent upperbound is  $|d_e| < 8.7 \cdot 10^{-16} e \text{ fm}$  [11], derived from the EDM of the ThO molecule.

In this context, there are proposals for the direct measurement of EDMs of electrons, single nucleons and light nuclei in dedicated storage rings [12–16]. This new approach plans to reach an accuracy of  $\sim 10^{-16} e \text{ fm}$ , improving the sensitivity in particular in the hadronic sector. Any measurement of a non-vanishing EDM of this magnitude would be the evidence of TRV beyond CKM effects. However, a single measurement will not be sufficient to identify the source of TRV. For this reason, the measurement of EDM of various light nuclei such as  $^2\text{H}$ ,  $^3\text{H}$  and  $^3\text{He}$  can impose constraints on the TRV sources.

On the other hand, also spin rotation of polarized neu-

trons along the  $y$ -axis can be used as probe for TRV [17–21]. This explorative study is motivated by the new sensitivity reached by various cold neutron facilities such as the Los Alamos Neutron Science Center, the National Institute of Standards and Technology (NIST) Center for Neutron Research, and the Spallation Neutron Source (SNS) at Oak Ridge National Laboratory. Even if the sensitivity of the spin-rotation on TRV is far away from the present sensitivity of the EDM, this observable addresses the same physics of the EDM, posing, for the future, as a complementary and independent test for TRV in nuclei. Also other TRV observables in proton- and neutron-nucleus scattering have been proposed as probes of TRV effects [21–25].

The use of light nuclei to study TRV results to be advantageous because the nuclear physics of the systems is theoretically under control and so the TRV effects can be easily highlighted. In particular, the chiral effective field theory ( $\chi$ EFT) has provided a practical and successful scheme to study two and many-nucleon interactions [26, 27] and the interaction of electroweak probes with nuclei [28–34]. The  $\chi$ EFT approach is based on the observation that the chiral symmetry exhibited by QCD has a noticeable impact in the low-energy regime. Therefore, the form of the strong interactions of pions among themselves and other particles is severely constrained by the transformation properties of the fundamental Lagrangian under Lorentz, parity, time-reversal, and chiral symmetry [35, 36]. The Lagrangian terms can be organized as an expansion in powers of  $Q/\Lambda_\chi$ , where  $\Lambda_\chi \simeq 1 \text{ GeV}$  specifies the chiral symmetry breaking scale and  $Q$  is the exchanged pion momentum. Each term is associated to a low-energy constants (LECs) which are then determined by fits to experimental data.

The  $\chi$ EFT method permits to construct also an effective TRV Lagrangian treating all possible sources of TRV. The TRV Lagrangian induced by the  $\theta$ -term was derived in Refs. [37, 38]. Also BSM terms such as supersymmetry, multi-Higgs scenarios, left-right symmetric model *etc.* induce TRV operators at the quark-gluon level which appear at level of dimension six (see for example Ref. [39]). The  $\chi$ EFT Lagrangians for these sources

were derived in Refs. [38, 40–42]. This approach permits not only to determine the TRV interactions but also to estimate the chiral order of the LECs and their values as function of the fundamental parameters, providing a direct connection between the fundamental theories and the nuclear observables [37, 38, 40]. To be noticed that the chiral order of the Lagrangian terms, which is determined by the products of the chiral order of the dynamical part and that of the LECs, really depends on the particular source of TRV. Therefore, when the LECs will be determined experimentally it will be possible to identify the dynamical properties of the TRV source [42, 43].

Starting from the TRV Lagrangian, de Vries *et al.* [44] and also Baisou *et al.* [45] derived the chiral potential up to next-to-next leading order (N2LO) including only nucleon-pion interaction and contact interactions. In both works also the electromagnetic currents which play a role at N2LO for the EDM were derived but only in Ref. [45] they were used to evaluate the EDM of the deuteron. In Ref. [46] the calculation of the EDM of  $^2\text{H}$ ,  $^3\text{H}$  and  $^3\text{He}$  was performed using only the one-pion-exchange part of the TRV potential coupled with phenomenological potential for the parity conserving (PC) part of the interaction.

Subsequent works showed the presence in the TRV Lagrangian of a three-pion term [38], which was included in the calculation for the first time by Baisou *et al.* [47]. This term generates at next-to-leading order (NLO) also a TRV three body force, which contribution to the  $^3\text{H}$  and  $^3\text{He}$  EDM was found to be smaller than expected by the chiral counting. The calculation reported in Ref. [47] was also the first to use a complete chiral approach including the TRV potential up to NLO and the PC potential up to N2LO.

The aim of this work is twofold: First, the construction of a TRV potential up to N2LO considering all possible TRV interaction terms in the  $\chi\text{EFT}$  without making any assumption for the chiral order of the LECs. In this way all possible sources of TRV can be studied just setting the LECs to their estimated values and turning on and off the various terms in the Lagrangian. The second is the study of the EDM of  $^2\text{H}$ ,  $^3\text{H}$  and  $^3\text{He}$ , providing a suitable framework for the future determination of the LECs. In our calculation the contribution of the TRV three-body force is found to be sizably larger than reported in Ref. [47].

Finally, it is worthy to mention that exists a different approach to the derivation of the TRV nuclear forces based on meson-exchange model [19]. This model includes pion and vector-meson exchange with 10 unknown meson constants. Such a theory, which has a wider energy range of validity but it is less systematic and with no direct connection with the fundamental Lagrangian, has been used to study the EDM of light nuclei [19, 48–50] and the neutron spin rotation  $\vec{n} - \vec{p}$  [20] and  $\vec{n} - \vec{d}$  [19, 22] scattering.

The present paper is organized as follows. In Sec. II we will present the TRV chiral Lagrangian up to order  $Q^2$

relevant for the calculation of the TRV potential, while in Sec. III we derive the TRV potential at N2LO. In Sec. IV, we report the results obtained for the EDM of  $^2\text{H}$ ,  $^3\text{H}$  and  $^3\text{He}$  using the N2LO potential. Finally, in Sec. V we present our conclusions and perspectives. The technical details relative to the contributions of the various diagrams, and of the derivation of the potential in configuration space are given in Appendices A, B and C. Moreover, in Appendix D we will give some details of the calculation of the trinucleon wave function negative-parity component and about the convergence of the TRV three body force contribution.

## II. THE TRV LAGRANGIAN

The various possible sources of TRV in SM induce a TRV  $NN$  and  $NNN$  potential. This potential can be constructed starting from a pion-nucleon effective Lagrangian which includes, in principle, an infinite set of terms which violates the chiral symmetry as the fundamental (quark-level) Lagrangian. The effective Lagrangian can be ordered by a power counting scheme which permits to select the most important interactions. In literature the chiral order of the TRV Lagrangian is determined by considering the estimated order of the LECs [37, 38, 40] which, however, is source dependent.

In this section we present only the TRV Lagrangian terms which can give some contribution to TRV  $NN$  and  $NNN$  potential up to N2LO in terms of pion field. In order to remain source independent we consider isoscalar, isovector and isotensor terms and we determine the chiral order of the TRV Lagrangian considering only the dynamical part. Namely, in the following we will consider all the TRV LECs to be equally important. To deal with a specific source of TRV, it will be sufficient to set some of the LECs to be zero, etc. At order  $Q^0$  the TRV pion-nucleon Lagrangian includes three terms [37, 38]

$$\mathcal{L}_{\text{TRV}}^{\pi N(0)} = g_0 \bar{\psi} \vec{\pi} \cdot \vec{\tau} \psi + g_1 \bar{\psi} \pi_3 \psi + g_2 \bar{\psi} \pi_3 \tau_3 \psi, \quad (1)$$

where  $\vec{\pi}$  is the pion field and  $\psi$  is the nucleon field. To be noticed that the isotensor term is usually considered of higher order. At the same order a purely pionic interaction appears [38], which reads

$$\mathcal{L}_{\text{TRV}}^{3\pi(0)} = M \Delta_3 \pi_3 \pi^2, \quad (2)$$

where  $M = 938.88$  MeV is the average nucleon mass. At order  $Q$  we have only one term that can give contribution to the potential up to N2LO and it reads, given explicitly as,

$$\mathcal{L}_{\text{TRV}}^{\pi N(1)} = \frac{g_V^{(1)}}{2Mf_\pi} [\bar{\psi} \partial_\mu (\vec{\pi} \times \vec{\tau})_3 \partial^\mu \psi + \text{h.c.}], \quad (3)$$

while no Lagrangian terms for the pure pionic interaction are allowed. At order  $Q^2$  we get six new contributions,

$$\mathcal{L}_{\text{TRV}}^{\pi N(2)} = \frac{g_{S1}^{(2)}}{f_\pi^2} \bar{\psi} \partial_\mu \partial^\mu (\pi \cdot \tau) \psi$$

$$\begin{aligned}
& + \frac{g_{S2}^{(2)}}{2M^2 f_\pi^2} [\bar{\psi} \partial_\mu \partial_\nu (\pi \cdot \tau) \partial^\mu \partial^\nu \psi + \text{h.c.}] \\
& + \frac{g_{V1}^{(2)}}{f_\pi^2} \bar{\psi} \partial_\mu \partial^\mu \pi_3 \psi \\
& + \frac{g_{V2}^{(2)}}{2M^2 f_\pi^2} [\bar{\psi} \partial_\mu \partial_\nu \pi_3 \partial^\mu \partial^\nu \psi + \text{h.c.}] \\
& + \frac{g_{T1}^{(2)}}{f_\pi^2} \bar{\psi} \partial_\mu \partial^\mu \pi_3 \tau_3 \psi \\
& + \frac{g_{T2}^{(2)}}{2M^2 f_\pi^2} [\bar{\psi} \partial_\mu \partial_\nu \pi_3 \tau_3 \partial^\mu \partial^\nu \psi + \text{h.c.}] , \quad (4)
\end{aligned}$$

where  $S, V, T$  stand for isoscalar, isovector and isotensor respectively and  $f_\pi \simeq 92$  MeV is the pion decay constant. The three-pion interaction that appears at this level gives contributions of order  $Q^2$  to the TRV nuclear potential which is beyond our purpose, therefore we do not consider it. The Lagrangian contains also four-nucleon contact terms  $\mathcal{L}_{\text{TRV}}^{\text{CT}}$  representing interactions originating from excitation of resonances and exchange of heavy mesons. At lowest order  $\mathcal{L}_{\text{TRV}}^{\text{CT}}$  contains only five independent four-nucleon contact terms with a single gradient.

In the following we also need the PC Lagrangian up to N2LO:

$$\mathcal{L}^{PC} = \mathcal{L}_{\pi\pi}^{(2)} + \dots + \mathcal{L}_{N\pi}^{(1)} + \mathcal{L}_{N\pi}^{(2)} + \mathcal{L}_{N\pi}^{(3)} + \dots + \mathcal{L}_{CT}^{PC} , \quad (5)$$

$$\mathcal{L}_{\pi\pi}^{(2)} = \frac{f_\pi^2}{4} \langle \nabla_\mu U^\dagger \nabla^\mu U + \chi^\dagger U + \chi U^\dagger \rangle , \quad (6)$$

$$\mathcal{L}_{N\pi}^{(1)} = \bar{\psi} \left( i \gamma^\mu D_\mu - M + \frac{g_A}{2} \gamma^\mu \gamma^5 u_\mu \right) \psi , \quad (7)$$

$$\begin{aligned}
\mathcal{L}_{N\pi}^{(2)} = & c_1 \bar{\psi} \langle \chi_+ \rangle \psi - \frac{c_2}{8M^2} [\bar{\psi} \langle u_\mu u_\nu \rangle D^\mu D^\nu \psi + \text{h.c.}] \\
& + c_3 \bar{\psi} \frac{1}{2} \langle u_\mu u^\mu \rangle \psi + c_4 \bar{\psi} \frac{i}{4} [u_\mu, u_\nu] \sigma^{\mu\nu} \psi + \dots , \quad (8)
\end{aligned}$$

$$\begin{aligned}
\mathcal{L}_{N\pi}^{(3)} = & d_{16} \bar{\psi} \frac{1}{2} \gamma^\mu \gamma^5 u_\mu \langle \chi_+ \rangle \psi \\
& + d_{18} \bar{\psi} \frac{i}{2} \gamma^\mu \gamma^5 [D_\mu, \chi_-] \psi + \dots , \quad (9)
\end{aligned}$$

where the building blocks  $U, u_\mu, \chi_+, \chi_-$  and the covariant derivative  $D_\mu$  are defined in Ref. [51]. We have omitted all the terms not relevant in the present work (for the complete expression for Lagrangian  $\mathcal{L}_{N\pi}^{(2)}$  and  $\mathcal{L}_{N\pi}^{(3)}$  in Ref. [52]). Four-nucleon contact terms (see, for example, Refs.[53, 54]) are lumped into  $\mathcal{L}_{CT}^{PC}$ . The parameters  $c_1, c_2, c_3, c_4, d_{16}$ , and  $d_{18}$  are LECs entering the PC Lagrangian. All the constants entering the terms discussed in this section have to be considered as “bare” parameters (i.e. unrenormalized).

### III. THE TRV POTENTIAL UP TO ORDER Q

In this section, we discuss the derivation of the TRV  $NN$  and  $NNN$  potential at N2LO. We provide, order by

order in power counting the formal expressions for it in terms of the time-ordered perturbation theory (TOPT) amplitudes, following the scheme presented in Ref. [51]. Then, the various diagrams associated with these amplitudes are discussed (additional details are given in Appendix B). We will give also some hints in the renormalization of the coupling constants.

#### A. From amplitudes to potentials

We start considering the conventional  $NN$  scattering amplitude  $\langle N'N'|T|NN \rangle$ , where  $|NN \rangle$  and  $|N'N' \rangle$  represent the initial and final two nucleon state and  $T$  can be written as,

$$T = H_I \sum_{n=1}^{\infty} \left( \frac{1}{E_i - H_0 + i\eta} H_I \right)^{n-1} , \quad (10)$$

where  $E_i$  is the initial energy of the two nucleons,  $H_0$  is the Hamiltonian describing free pions and nucleons, and  $H_I$  is the Hamiltonian describing interactions among these particles. To be noticed that in Eq. (10) the interaction Hamiltonian  $H_I$  is in the Schrödinger picture and that, at the order of interest here, it follows simply from  $H_I = - \int d\mathbf{x} \mathcal{L}_I(t=0, \mathbf{x})$ , where  $\mathcal{L}_I$  is the interaction Lagrangian in interaction picture. Vertices from  $H_I$  are listed in Appendix A.

The  $NN$  scattering amplitude can be organized as an expansion in powers of  $Q/\Lambda_\chi \ll 1$ , where  $\Lambda_\chi \simeq 1$  GeV is the typical hadronic mass scale,

$$\langle N'N'|T|NN \rangle = \sum_n T^{(n)} , \quad (11)$$

where  $T^{(n)} \sim Q^n$ .

The  $T$  matrix in Eq. (11) is generated, order by order in the power counting, by the  $NN$  potential  $V$  from iterations of it in the Lippmann-Schwinger (LS) equation,

$$V + V G_0 V + V G_0 V G_0 V + \dots , \quad (12)$$

where  $G_0$  denotes the free two-nucleon propagator. If we assume that,

$$\langle N'N'|V|NN \rangle = \sum_n V^{(n)} , \quad (13)$$

with  $V^{(n)}$  of order  $Q^n$ , it is possible to assign to any  $T^{(n)}$  the terms in the LS equation that are of the same order. Generally in term like  $[V^{(m)} G_0 V^{(n)}]$  is of order  $Q^{m+n+1}$  because  $G_0$  is of order  $Q^{-2}$  and the implicit loop integration brings a factor  $Q^3$  (for a more detailed discussion, see Ref. [33]).

In our case the two nucleons interact via a PC potential plus a very small TRV component. The  $\chi$ EFT Lagrangian implies the following expansion in powers of  $Q$  for  $T = T_{PC} + T_{TRV}$ :

$$T_{PC} = T_{PC}^{(0)} + T_{PC}^{(1)} + T_{PC}^{(2)} + \dots , \quad (14)$$

$$T_{TRV} = T_{TRV}^{(-1)} + T_{TRV}^{(0)} + T_{TRV}^{(1)} + \dots \quad (15)$$

Assuming that the potential  $V = V_{PC} + V_{TRV}$  have a similar expansion,

$$V_{PC} = V_{PC}^{(0)} + V_{PC}^{(1)} + V_{PC}^{(2)} + \dots \quad (16)$$

$$V_{TRV} = V_{TRV}^{(-1)} + V_{TRV}^{(0)} + V_{TRV}^{(1)} + \dots, \quad (17)$$

we can match order by order the  $T$  and the terms in the LS equation obtaining the form definition of the TRV  $NN$  potential from the scattering amplitude,

$$V_{TRV}^{(-1)} = T_{TRV}^{(-1)}, \quad (18)$$

$$V_{TRV}^{(0)} = T_{TRV}^{(0)} - \left[ V_{TRV}^{(-1)} G_0 V_{PC}^{(0)} \right] - \left[ V_{PC}^{(0)} G_0 V_{TRV}^{(-1)} \right], \quad (19)$$

$$\begin{aligned} V_{TRV}^{(1)} = T_{TRV}^{(1)} &- \left[ V_{TRV}^{(0)} G_0 V_{PC}^{(0)} \right] - \left[ V_{PC}^{(0)} G_0 V_{TRV}^{(0)} \right] \\ &- \left[ V_{TRV}^{(-1)} G_0 V_{PC}^{(1)} \right] - \left[ V_{PC}^{(1)} G_0 V_{TRV}^{(-1)} \right] \\ &- \left[ V_{TRV}^{(-1)} G_0 V_{PC}^{(0)} G_0 V_{PC}^{(0)} \right] - \left[ V_{PC}^{(0)} G_0 V_{TRV}^{(-1)} G_0 V_{PC}^{(0)} \right] \\ &- \left[ V_{PC}^{(0)} G_0 V_{PC}^{(0)} G_0 V_{TRV}^{(-1)} \right]. \end{aligned} \quad (20)$$

The generalization for the  $NNN$  TRV potential is straightforward.

## B. The $NN$ TRV potential

We define the following momenta,

$$\mathbf{K}_j = (\mathbf{p}'_j + \mathbf{p}_j)/2, \quad \mathbf{k}_j = \mathbf{p}'_j - \mathbf{p}_j, \quad (21)$$

where  $\mathbf{p}_j$  and  $\mathbf{p}'_j$  are the initial and final momenta of nucleon  $j$ . From the overall momentum conservation  $\mathbf{p}_1 + \mathbf{p}_2 = \mathbf{p}'_1 + \mathbf{p}'_2$ , we can define  $\mathbf{k} = \mathbf{k}_1 = -\mathbf{k}_2$ . We also define  $\mathbf{K} = (\mathbf{K}_1 - \mathbf{K}_2)/2$ ,  $\mathbf{P} = \mathbf{p}_1 + \mathbf{p}_2 = \mathbf{K}_1 + \mathbf{K}_2$ , in this way is possible to write the TRV  $NN$  potential as,

$$V_{TRV}(\mathbf{k}, \mathbf{K}_1, \mathbf{K}_2) = V_{TRV}^{(c.m.)}(\mathbf{k}, \mathbf{K}) + V_{TRV}^{(P)}(\mathbf{k}, \mathbf{K}), \quad (22)$$

where the term  $V_{TRV}^{(P)}(\mathbf{k}, \mathbf{K})$  represents boost corrections to  $V_{TRV}^{(c.m.)}(\mathbf{k}, \mathbf{K})$  [55], the potential in the center-of-mass (c.m.) frame. Below we ignore these boost corrections and provide expressions for  $V_{TRV}^{(c.m.)}(\mathbf{k}, \mathbf{K})$  only.

The diagrams that give contribution to the  $NN$  TRV potential are shown in Fig. 1. We do not consider diagrams which give contribution only to the renormalization of the LECs. In this section we write the final expression of the  $NN$  TRV potential  $V_{TRV}^{(c.m.)}$  as,

$$\begin{aligned} V_{TRV}^{(c.m.)} = & V_{TRV}^{(OPE)} + V_{TRV}^{(TPE)} + V_{TRV}^{(3\pi,0)} + V_{TRV}^{(3\pi,1)} \\ & + V_{TRV}^{(RC)} + V_{TRV}^{(3\pi,RC)} + V_{TRV}^{(CT)}, \end{aligned} \quad (23)$$

namely as a sum of terms due to one-pion exchange (OPE), two-pion exchange (TPE), three-pion exchange at NLO ( $3\pi,0$ ) and at N2LO ( $3\pi,1$ ), relativistic corrections derived from the OPE (RC) and from the  $3\pi$ -exchange ( $3\pi,RC$ ), and contact contributions (CT). From

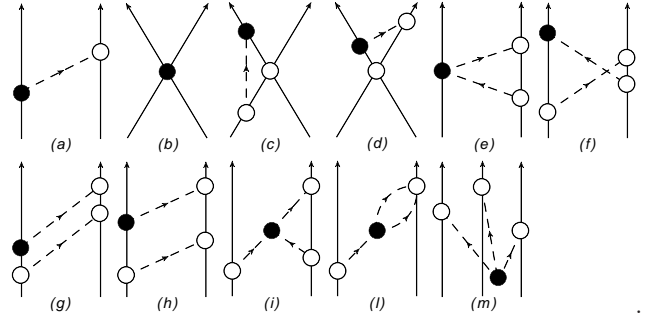


FIG. 1. Time-ordered diagrams contributing to the TRV potential (only a single time ordering is shown). Nucleons and pions are denoted by solid and dashed lines, respectively. The open (solid) circle represents a PC (TRV) vertex.

now on we define also  $g_0^* = g_0 + g_2/3$  (see Appendix B for details). The OPE term is the contribution of diagram (a) of order  $Q^{-1}$  (LO) and it reads,

$$\begin{aligned} V_{TRV}^{(OPE)} = & \frac{\bar{g}_A \bar{g}_0^*}{2\bar{f}_\pi} (\boldsymbol{\tau}_1 \cdot \boldsymbol{\tau}_2) \frac{i\mathbf{k} \cdot (\boldsymbol{\sigma}_1 - \boldsymbol{\sigma}_2)}{\omega_k^2} \\ & + \frac{\bar{g}_A \bar{g}_1}{4\bar{f}_\pi} \left[ (\tau_{1z} + \tau_{2z}) \frac{i\mathbf{k} \cdot (\boldsymbol{\sigma}_1 - \boldsymbol{\sigma}_2)}{\omega_k^2} \right. \\ & \quad \left. + (\tau_{1z} - \tau_{2z}) \frac{i\mathbf{k} \cdot (\boldsymbol{\sigma}_1 + \boldsymbol{\sigma}_2)}{\omega_k^2} \right] \\ & + \frac{\bar{g}_A \bar{g}_2}{6\bar{f}_\pi} (3\tau_{1z}\tau_{2z} - \boldsymbol{\tau}_1 \cdot \boldsymbol{\tau}_2) \frac{i\mathbf{k} \cdot (\boldsymbol{\sigma}_1 - \boldsymbol{\sigma}_2)}{\omega_k^2}, \end{aligned} \quad (24)$$

where there are an isoscalar, an isovector and an isotensor components and  $\bar{g}_0^* = \bar{g}_0 + \bar{g}_2/3$ . The coupling constants  $\bar{g}_A/\bar{f}_\pi$ ,  $\bar{g}_0^*$ ,  $\bar{g}_1$ ,  $\bar{g}_2$  are renormalized coupling constants, having reabsorbed the various infinities generated by loops and given as combinations of the “bare” LECs entering the Lagrangian. The expression for  $\bar{g}_A/\bar{f}_\pi$  is the same as reported in Ref. [51]. The LECs  $g_{S1}^{(2)}$ ,  $g_{S2}^{(2)}$ , etc. enter in Eq. (24) through the renormalized constants  $\bar{g}_0$ , etc. (see Appendix B for more details). Note that, as mentioned before, the correct expressions of the renormalized constants in term of the bare ones should contain also the contributions of additional diagrams not considered here (see Ref. [51] for the procedure to be followed for the PC and PV potentials, respectively).

The TPE term comes from the not singular contribution of panels (e)-(h) of Fig. 1, taking also into account the subtracting terms given in Eq. (20). As discussed in Appendix B this term has no isovector component, in agreement with the result reported in [44]. Therefore, as reported in Eqs. (B10) and (B17), we have,

$$\begin{aligned} V_{TRV}^{(TPE)} = & \frac{g_A g_0^*}{f_\pi \Lambda_\chi^2} \boldsymbol{\tau}_1 \cdot \boldsymbol{\tau}_2 i\mathbf{k} \cdot (\boldsymbol{\sigma}_1 - \boldsymbol{\sigma}_2) L(k) \\ & + \frac{g_A^3 g_0^*}{f_\pi \Lambda_\chi^2} \boldsymbol{\tau}_1 \cdot \boldsymbol{\tau}_2 i\mathbf{k} \cdot (\boldsymbol{\sigma}_1 - \boldsymbol{\sigma}_2) (H(k) - 3L(k)) \end{aligned}$$



$$\begin{aligned}
& -\frac{g_A g_2}{3f_\pi \Lambda_\chi^2} (3\tau_{1z}\tau_{2z} - \boldsymbol{\tau}_1 \cdot \boldsymbol{\tau}_2) i\mathbf{k} \cdot (\boldsymbol{\sigma}_1 - \boldsymbol{\sigma}_2) L(k) \\
& -\frac{g_A^3 g_2}{3f_\pi \Lambda_\chi^2} (3\tau_{1z}\tau_{2z} - \boldsymbol{\tau}_1 \cdot \boldsymbol{\tau}_2) \\
& \quad \times i\mathbf{k} \cdot (\boldsymbol{\sigma}_1 - \boldsymbol{\sigma}_2) (H(k) - 3L(k)) , \quad (25)
\end{aligned}$$

where the loop functions  $L(k)$  and  $H(k)$  are defined in Eqs. (B11) and (B18). In this and the following NLO and N2LO terms the bare coupling constants  $g_A$ ,  $f_\pi$ ,  $g_0^*$ , ... can be safely replaced by the corresponding physical (renormalized) values.

The  $3\pi$ -exchange term gives a NLO contribution through the diagram (i) of Fig. 1,

$$\begin{aligned}
V_{TRV}^{(3\pi,0)} = & -\frac{5g_A^3 \Delta_3 M}{4f_\pi \Lambda_\chi^2} \pi \left[ (\tau_{1z} + \tau_{2z}) \frac{i\mathbf{k} \cdot (\boldsymbol{\sigma}_1 - \boldsymbol{\sigma}_2)}{\omega_k^2} \right. \\
& \left. + (\tau_{1z} - \tau_{2z}) \frac{i\mathbf{k} \cdot (\boldsymbol{\sigma}_1 + \boldsymbol{\sigma}_2)}{\omega_k^2} \right] \\
& \times \left( \left(1 - \frac{2m_\pi^2}{s^2}\right) s^2 A(k) + m_\pi \right) , \quad (26)
\end{aligned}$$

where  $A(k)$  is defined in Eq. (B22). The expression obtained in Eq. (26) is in agreement with the expression derived in Refs. [38, 40].

The diagram in panel (l) of Fig. 1 contributes to  $V_{TRV}^{(3\pi)}$  at N2LO. The expression for this diagram is derived in Appendix B, here we report the final result only,

$$\begin{aligned}
V_{TRV}^{(3\pi,1)} = & \frac{5g_A \Delta_3 M c_1}{2f_\pi \Lambda_\chi^2} \left[ (\tau_{1z} + \tau_{2z}) i\mathbf{k} \cdot (\boldsymbol{\sigma}_1 - \boldsymbol{\sigma}_2) \right. \\
& \left. + (\tau_{1z} - \tau_{2z}) i\mathbf{k} \cdot (\boldsymbol{\sigma}_1 + \boldsymbol{\sigma}_2) \right] 4 \frac{m_\pi^2}{\omega_k^2} L(k) \\
& - \frac{5g_A \Delta_3 M c_2}{6f_\pi \Lambda_\chi^2} \left[ (\tau_{1z} + \tau_{2z}) i\mathbf{k} \cdot (\boldsymbol{\sigma}_1 - \boldsymbol{\sigma}_2) \right. \\
& \left. + (\tau_{1z} - \tau_{2z}) i\mathbf{k} \cdot (\boldsymbol{\sigma}_1 + \boldsymbol{\sigma}_2) \right] \left( 2L(k) + 6 \frac{m_\pi^2}{\omega_k^2} L(k) \right) \\
& - \frac{5g_A \Delta_3 M c_3}{4f_\pi \Lambda_\chi^2} \left[ (\tau_{1z} + \tau_{2z}) i\mathbf{k} \cdot (\boldsymbol{\sigma}_1 - \boldsymbol{\sigma}_2) \right. \\
& \left. + (\tau_{1z} - \tau_{2z}) i\mathbf{k} \cdot (\boldsymbol{\sigma}_1 + \boldsymbol{\sigma}_2) \right] \left( 3L(k) + 5 \frac{m_\pi^2}{\omega_k^2} L(k) \right) . \quad (27)
\end{aligned}$$

Note in Eq. (27) the presence of the  $c_1$ ,  $c_2$  and  $c_3$  LECs, which belong to the PC sector. In Eqs. (26) and (27) the  $\Delta_3$  is the renormalized LEC to the relative order of the expressions.

The  $V_{TRV}^{(RC)}$  term of the potential takes into account contributions from the RC of the vertices in the OPE of panel (a),

$$\begin{aligned}
V_{TRV}^{(RC)} = & \frac{g_A g_0^*}{8f_\pi M^2} \boldsymbol{\tau}_1 \cdot \boldsymbol{\tau}_2 \frac{1}{\omega_k^2} \\
& \times \left[ -\frac{i}{2} (8K^2 + k^2) \mathbf{k} \cdot (\boldsymbol{\sigma}_1 - \boldsymbol{\sigma}_2) \right.
\end{aligned}$$

$$\begin{aligned}
& \left. + \mathbf{k} \cdot \boldsymbol{\sigma}_1 (\mathbf{k} \times \mathbf{K}) \cdot \boldsymbol{\sigma}_2 - \mathbf{k} \cdot \boldsymbol{\sigma}_2 (\mathbf{k} \times \mathbf{K}) \cdot \boldsymbol{\sigma}_1 \right] \\
& + \frac{g_A g_1}{16f_\pi M^2} \frac{1}{\omega_k^2} \\
& \times \left\{ (\tau_{1z} - \tau_{2z}) \left[ -\frac{i}{2} (8K^2 + k^2) \mathbf{k} \cdot (\boldsymbol{\sigma}_1 + \boldsymbol{\sigma}_2) \right. \right. \\
& \left. \left. + \mathbf{k} \cdot \boldsymbol{\sigma}_1 (\mathbf{k} \times \mathbf{K}) \cdot \boldsymbol{\sigma}_2 + \mathbf{k} \cdot \boldsymbol{\sigma}_2 (\mathbf{k} \times \mathbf{K}) \cdot \boldsymbol{\sigma}_1 \right] \right. \\
& \left. + (\tau_{1z} + \tau_{2z}) \left[ -\frac{i}{2} (8K^2 + k^2) \mathbf{k} \cdot (\boldsymbol{\sigma}_1 - \boldsymbol{\sigma}_2) \right. \right. \\
& \left. \left. + \mathbf{k} \cdot \boldsymbol{\sigma}_1 (\mathbf{k} \times \mathbf{K}) \cdot \boldsymbol{\sigma}_2 - \mathbf{k} \cdot \boldsymbol{\sigma}_2 (\mathbf{k} \times \mathbf{K}) \cdot \boldsymbol{\sigma}_1 \right] \right\} \\
& + \frac{g_A g_2}{24f_\pi M^2} (3\tau_{1z}\tau_{2z} - \boldsymbol{\tau}_1 \cdot \boldsymbol{\tau}_2) \frac{1}{\omega_k^2} \\
& \times \left[ -\frac{i}{2} (8K^2 + k^2) \mathbf{k} \cdot (\boldsymbol{\sigma}_1 - \boldsymbol{\sigma}_2) \right. \\
& \left. + \mathbf{k} \cdot \boldsymbol{\sigma}_1 (\mathbf{k} \times \mathbf{K}) \cdot \boldsymbol{\sigma}_2 - \mathbf{k} \cdot \boldsymbol{\sigma}_2 (\mathbf{k} \times \mathbf{K}) \cdot \boldsymbol{\sigma}_1 \right] , \quad (28)
\end{aligned}$$

where, as for the OPE, we have an isoscalar, an isovector and an isotensor term. Also the diagram of Fig. 1 (i) gives a contribution to the at N2LO, both from the RC of the vertices, and from NLO in the pion propagators (see Appendix B). The final expression we obtain is

$$\begin{aligned}
V_{TRV}^{(3\pi,RC)} = & -\frac{5g_A^3 \Delta_3}{16f_\pi \Lambda_\chi^2} \left[ (\tau_{1z} + \tau_{2z}) i\mathbf{k} \cdot (\boldsymbol{\sigma}_1 - \boldsymbol{\sigma}_2) \right. \\
& \left. + (\tau_{1z} - \tau_{2z}) i\mathbf{k} \cdot (\boldsymbol{\sigma}_1 + \boldsymbol{\sigma}_2) \right] \\
& \times \left( \frac{25}{6} L(k) - \frac{7}{2} \frac{m_\pi^2}{\omega_k^2} L(k) + 2 \frac{m_\pi^2}{\omega_k^2} H(k) \right) \\
& - \frac{25g_A^3 \Delta_3}{12f_\pi \Lambda_\chi^2} \frac{1}{\omega_k^2} \left\{ (\tau_{1z} + \tau_{2z}) \left[ \mathbf{k} \cdot \boldsymbol{\sigma}_1 (\mathbf{k} \times \mathbf{K}) \cdot \boldsymbol{\sigma}_2 \right. \right. \\
& \left. \left. + \mathbf{k} \cdot \boldsymbol{\sigma}_2 (\mathbf{k} \times \mathbf{K}) \cdot \boldsymbol{\sigma}_1 \right] + (\tau_{1z} - \tau_{2z}) \right. \\
& \left. \times \left[ \mathbf{k} \cdot \boldsymbol{\sigma}_1 (\mathbf{k} \times \mathbf{K}) \cdot \boldsymbol{\sigma}_2 - \mathbf{k} \cdot \boldsymbol{\sigma}_2 (\mathbf{k} \times \mathbf{K}) \cdot \boldsymbol{\sigma}_1 \right] \right\} , \quad (29)
\end{aligned}$$

where in Eqs. (28) and (29) the TRV coupling constants are renormalized to order  $Q^2$ .

Last, the potential  $V_{TRV}^{(CT)}$ , derived from the  $NN$  contact diagrams (b) of Fig. 1, reads

$$\begin{aligned}
V_{TRV}^{(CT)} = & \frac{1}{\Lambda_\chi^2 f_\pi} \left\{ \overline{C}_1 i\mathbf{k} \cdot (\boldsymbol{\sigma}_1 - \boldsymbol{\sigma}_2) \right. \\
& + \overline{C}_2 i\mathbf{k} \cdot (\boldsymbol{\sigma}_1 - \boldsymbol{\sigma}_2) \boldsymbol{\tau}_1 \cdot \boldsymbol{\tau}_2 \\
& + \frac{\overline{C}_3}{2} \left[ i\mathbf{k} \cdot (\boldsymbol{\sigma}_1 - \boldsymbol{\sigma}_2) (\tau_{z1} + \tau_{z2}) \right. \\
& \left. - i\mathbf{k} \cdot (\boldsymbol{\sigma}_1 + \boldsymbol{\sigma}_2) (\tau_{z1} - \tau_{z2}) \right] \\
& + \frac{\overline{C}_4}{2} \left[ i\mathbf{k} \cdot (\boldsymbol{\sigma}_1 - \boldsymbol{\sigma}_2) (\tau_{z1} + \tau_{z2}) \right. \\
& \left. + i\mathbf{k} \cdot (\boldsymbol{\sigma}_1 + \boldsymbol{\sigma}_2) (\tau_{z1} - \tau_{z2}) \right] \\
& \left. + \overline{C}_5 i\mathbf{k} \cdot (\boldsymbol{\sigma}_1 - \boldsymbol{\sigma}_2) (3\tau_{z1}\tau_{z2} - \boldsymbol{\tau}_1 \cdot \boldsymbol{\tau}_2) \right\} . \quad (30)
\end{aligned}$$

Above  $\overline{C}_1$ ,  $\overline{C}_2$ ,  $\overline{C}_3$ ,  $\overline{C}_4$  and  $\overline{C}_5$  are renormalized LECs since they have reabsorbed various singular terms coming from the TPE diagrams,  $3\pi$  diagrams and the relativistic corrections. Note that it is possible to write ten operators which can enter  $V_{TRV}^{(CT)}$  at order  $Q$  but only five of them are independent. In this work we have chosen to write the operators in term of  $\mathbf{k}$ , so that the  $r$ -space version of  $V_{TRV}^{(CT)}$  will assume a simple local form with no gradients. We want also to remark that the  $C_2$ ,  $C_4$  and  $C_5$  LECs are needed in order to reabsorb the divergences coming from the TPE and  $3\pi$  exchange diagrams.

In the calculation of the EDM in Sec. IV, the configuration space version of the potential is needed. This formally follows from

$$\langle \mathbf{r}'_1 \mathbf{r}'_2 | V | \mathbf{r}_1 \mathbf{r}_2 \rangle = \delta(\mathbf{R} - \mathbf{R}') \int \frac{d^3 k}{(2\pi)^3} \frac{d^3 K}{(2\pi)^3} \times e^{i(\mathbf{K} + \mathbf{k}/2) \cdot \mathbf{r}'} V(\mathbf{k}, \mathbf{K}) e^{-i(\mathbf{K} - \mathbf{k}/2) \cdot \mathbf{r}}, \quad (31)$$

where  $\mathbf{r} = \mathbf{r}_1 - \mathbf{r}_2$  and  $\mathbf{R} = (\mathbf{r}_1 + \mathbf{r}_2)/2$ , and similarly for the primed variables. In order to carry out the Fourier transforms above, the integrand is regularized by including a cutoff of the form

$$C_\Lambda(k) = e^{-(k/\Lambda)^4}, \quad (32)$$

where the cutoff parameter  $\Lambda$  is taken in the range 450–550 MeV. With such a choice the  $V_{TRV}^{(OPE)}$ ,  $V_{TRV}^{(TPE)}$ ,  $V_{TRV}^{(3\pi,0)}$ ,  $V_{TRV}^{(3\pi,1)}$ , and  $V_{TRV}^{(CT)}$  components of the resulting potential are local, i.e.,  $\langle \mathbf{r}'_1 \mathbf{r}'_2 | V | \mathbf{r}_1 \mathbf{r}_2 \rangle = \delta(\mathbf{R} - \mathbf{R}') \delta(\mathbf{r} - \mathbf{r}') V(\mathbf{r})$ , while the RC component contains mild non-localities associated with linear and quadratic terms in the relative momentum operator  $-i\nabla$ . Explicit expressions for all these components are listed in Appendix C 1.

### C. The $NNN$ TRV potential

The  $3\pi$  TRV vertex gives rise to a three body contribution through the diagram (m) in Fig. 1. The lowest contribution appears at NLO while at N2LO the various time ordering cancel out (see Appendix B). The final expression for the NLO of the  $NNN$  TRV potential is,

$$V_{TRV}^{NNN} = \frac{\Delta_3 g_A^3 M}{4f_\pi^3} (\boldsymbol{\tau}_1 \cdot \boldsymbol{\tau}_2 \tau_{3z} + \boldsymbol{\tau}_1 \cdot \boldsymbol{\tau}_3 \tau_{2z} + \boldsymbol{\tau}_2 \cdot \boldsymbol{\tau}_3 \tau_{1z}) \times \frac{(i\mathbf{k}_1 \cdot \boldsymbol{\sigma}_1)(i\mathbf{k}_2 \cdot \boldsymbol{\sigma}_2)(i\mathbf{k}_3 \cdot \boldsymbol{\sigma}_3)}{\omega_{k_1}^2 \omega_{k_2}^2 \omega_{k_3}^2}, \quad (33)$$

which is in agreement with the expression of Ref. [38, 40].

Also in this case we need the Fourier transform of the potential. Using the overall momentum conservation  $\mathbf{p}_1 + \mathbf{p}_2 + \mathbf{p}_3 = \mathbf{p}'_1 + \mathbf{p}'_2 + \mathbf{p}'_3$ , which give us that  $\mathbf{k}_3 = -\mathbf{k}_1 - \mathbf{k}_2$ , and defining  $\mathbf{Q} = \mathbf{k}_1 + \mathbf{k}_2$  and  $\mathbf{q} = \mathbf{k}_1 - \mathbf{k}_2$  the Fourier transform becomes,

$$\langle \mathbf{r}'_1 \mathbf{r}'_2 \mathbf{r}'_3 | V | \mathbf{r}_1 \mathbf{r}_2 \mathbf{r}_3 \rangle = \delta(\mathbf{r}_1 - \mathbf{r}'_1) \delta(\mathbf{r}_2 - \mathbf{r}'_2) \delta(\mathbf{r}_3 - \mathbf{r}'_3)$$

$$\times \int \frac{d^3 q}{(2\pi)^3} \frac{d^3 Q}{(2\pi)^3} V(\mathbf{q}, \mathbf{Q}) e^{-i(\mathbf{q}/2) \cdot \mathbf{x}_2} e^{-i\mathbf{Q} \cdot \mathbf{x}_1}, \quad (34)$$

where  $\mathbf{x}_1 = \mathbf{r}_2 - \mathbf{r}_1$  and  $\mathbf{x}_2 = \mathbf{r}_3 - (\mathbf{r}_1 + \mathbf{r}_2)/2$ . Note that with this choice of  $\mathbf{Q}$  and  $\mathbf{q}$ , the form of the Jacobi vectors appear automatically. We use the regularization function reported in Eq. (32), where we replace  $k$  with  $Q$ , namely,

$$C_\Lambda(Q) = e^{-(Q/\Lambda)^4}, \quad (35)$$

which gives a local form of the  $NNN$  TRV potential. A complete description of how to carry out the integration in the Fourier transform is given in Appendix C 2.

## IV. RESULTS

In this section, we report results for the EDM of  ${}^2\text{H}$ ,  ${}^3\text{H}$  and  ${}^3\text{He}$ . Hereafter, we do not use the barred notation for the renormalized LECs but all the coupling constant must be considered as renormalized. The calculations are based on the TRV  $NN$  potential derived in the previous section (and summarized in Appendix B) and on the (strong interaction) PC  $NN$  potential obtained by Entem and Machleidt at next-to-next-to-next-to-next-to-leading order (N4LO) [26]. These potentials are regularized with a cutoff function depending on a parameter  $\Lambda$ ; its functional form, however, is different from the adopted here for  $V_{TRV}$ . Below we consider the versions with  $\Lambda = 450$  MeV, 500 MeV, and 550 MeV. The calculations of  ${}^3\text{H}$  and  ${}^3\text{He}$  EDMs also include the  $NNN$  TRV nuclear potential derived in Sec. III C and the PC  $NNN$  potential derived in  $\chi\text{EFT}$  at N2LO. As for the  $NN$  PC potential, it depends on a cutoff parameter  $\Lambda$  which is chosen to be consistent with those in the PC and TRV  $NN$  potentials. The three-nucleon PC potential depends, in addition, on two unknown LECs, denoted as  $c_D$  and  $c_E$  and also on the LECs  $c_1$ ,  $c_3$  and  $c_4$ . In this work, we use the values reported in Table III of Ref. [56]. The  $V_{TRV}^{(3\pi,1)}$  term of the TRV potential depends on the LECs  $c_1$ ,  $c_2$  and  $c_3$  which are taken from Table II of Ref. [26] and summarized here in Table I. In the following the values  $g_A = 1.267$  and

PC interactions	$c_1$	$c_2$	$c_3$
N2LO	-0.74	-	-3.61
N3LO	-1.07	3.20	-5.32
N4LO	-1.10	3.57	-5.54

TABLE I. Values of the coefficients and  $c_1$ ,  $c_2$ ,  $c_3$  in unit of  $\text{GeV}^{-1}$  taken from Ref. [26].

$f_\pi = 92.4$  MeV are adopted.

This section is organized as follows. In Sec. IV A, we present the general expression for the EDM operator and the results for the deuteron EDM, while in Sec. IV B we present the calculation of the  ${}^3\text{H}$  and  ${}^3\text{He}$  EDMs.

### A. Deuteron EDM

The EDM operator  $\hat{D}$  is composed by two parts,

$$\hat{D} = \hat{D}_{\text{PC}} + \hat{D}_{\text{TRV}}. \quad (36)$$

The  $\hat{D}_{\text{PC}}$  receives contribution at LO from the nuclear EDM polarization operator

$$\hat{D}_{\text{PC}} = e \sum_i \frac{1 + \tau_z(i)}{2} \mathbf{r}_i, \quad (37)$$

where  $e > 0$  is the electric unit charge,  $\tau_z(i)$  and  $\mathbf{r}_i$  are the  $z$  component of the isospin and the position of the  $i$ -th particle. The  $\hat{D}_{\text{TRV}}$  LO contribution comes from the intrinsic nucleon EDM,

$$\hat{D}_{\text{TRV}} = \frac{1}{2} \sum_i [(d_p + d_n) + (d_p - d_n)\tau_z(i)] \boldsymbol{\sigma}(i), \quad (38)$$

where  $d_p$  and  $d_n$  are the EDM of proton and neutron respectively and  $\boldsymbol{\sigma}(i)$  is the spin operator which act on the  $i$ -th particle. As discussed in Refs. [45, 46] both the  $\hat{D}_{\text{PC}}$  and  $\hat{D}_{\text{TRV}}$  receive contributions from transition currents at N2LO. Of course, a complete treatment of the EDM up to N2LO needs to take care of them but hereafter we neglect their contribution, showing only the effects of N2LO TRV potential. In future work we plan to include the N2LO current contributions in the calculations.

The nucleon EDM of an  $A$  nucleus can be expressed as

$$\begin{aligned} d^A &= \langle \psi_+^A | \hat{D}_{\text{TRV}} | \psi_+^A \rangle + 2 \langle \psi_+^A | \hat{D}_{\text{PC}} | \psi_-^A \rangle \\ &\equiv d_{\text{TRV}}^A + d_{\text{PC}}^A, \end{aligned} \quad (39)$$

where  $|\psi_+^A\rangle$  ( $|\psi_-^A\rangle$ ) is defined to be the even-parity (odd-parity) component of the wave function. In general, due to the smallness of the LECs, the EDM can be expressed as linear on the TRV LECs,

$$\begin{aligned} d_{\text{TRV}}^A &= d_p a_p + d_n a_n \\ d_{\text{PC}}^A &= g_0 a_0 + g_1 a_1 + g_2 a_2 + \Delta_3 a_\Delta \\ &\quad + C_1 A_1 + C_2 A_2 + C_3 A_3 + C_4 A_4 + C_5 A_5, \end{aligned} \quad (40)$$

where the  $a_i$  for  $i = 0, 1, 2$ ,  $a_\Delta$ ,  $A_i$  for  $i = 1, \dots, 5$  and  $a_p$ ,  $a_n$  are numerical coefficients independent on the LECs values (however, they do depend on the cutoff  $\Lambda$  in the PC and TRV chiral potentials).

We evaluate also the theoretical errors associated with the chiral expansion of the nuclear potential. We express the error on the numerical coefficients for the deuteron as,

$$(\delta a_i)^2 = (\delta a_i^{\text{PC}})^2 + (\delta a_i^{\text{TRV}})^2, \quad (42)$$

where  $\delta a_i^{\text{PC}}$  is the error associated to the chiral expansion of the PC potential and  $\delta a_i^{\text{TRV}}$  the error associated with the chiral expansion of the TRV potential. Both the contributions were evaluated following the prescriptions of Epelbaum *et al.* [27] where as reference momentum

$\Lambda(\text{MeV})$	450	500	550
$a_n(a_p)$	$0.934 \pm 0.001$	$0.939 \pm 0.001$	$0.938 \pm 0.001$
$a_1$	$0.192 \pm 0.006$	$0.197 \pm 0.004$	$0.194 \pm 0.003$
$a_\Delta$	$-0.306 \pm 0.174$	$-0.341 \pm 0.153$	$-0.349 \pm 0.137$
$A_3$	$0.013 \pm 0.004$	$0.013 \pm 0.004$	$0.013 \pm 0.004$
$A_4$	$-0.013 \pm 0.004$	$-0.013 \pm 0.004$	$-0.013 \pm 0.004$

TABLE II. Values of the deuteron coefficients  $a_n$  and  $a_p$  in units of  $d_p$  and  $d_n$  and of  $a_1$ ,  $a_\Delta$ ,  $A_3$ ,  $A_4$  in units of  $e$  fm for the three different choices of cutoff parameters  $\Lambda$ .

in the calculation of the errors we used the mass of the pion. It is straightforward to understand that the errors are dominated by the TRV part because we are using the N2LO potential for it and the N4LO potential for the PC part.

The coefficients for the deuteron, evaluated with the N4LO PC potential and the N2LO TRV potential and the associated errors for the three different choices of the cutoff parameters, are given in Table II. The coefficients  $a_p$  and  $a_n$  multiplying the intrinsic neutron and proton EDM, as already pointed out first in Ref. [49] and then in Ref. [47], are given by,

$$a_n = a_p = \left(1 - \frac{3}{2} P_D\right), \quad (43)$$

where  $P_D$  is the percentage of D-wave present in the deuteron wave function. The values of  $a_n$  and  $a_p$  obtained using the Entem and Machleidt at N4LO for three different choices of the cut off are reported in Table II. The operator  $\hat{D}_{\text{PC}}$  for the deuteron reduces to  $\hat{D}_{\text{PC}} = (\tau_z(1) - \tau_z(2))\mathbf{r}$  therefore  $d_{\text{PC}}^2$  in Eq. (41) receives contribution only from the component  $^3P_1$  which has  $T = 1$ . This component is generated by the TRV potential components proportional to  $(\boldsymbol{\sigma}_1 + \boldsymbol{\sigma}_2)$ , namely those proportional to  $g_1$ ,  $\Delta_3$ ,  $C_3$  and  $C_4$ .

The coefficient  $a_\Delta$  can be written as,

$$a_\Delta = a_\Delta(0) + (c_1 a_\Delta(1) + c_2 a_\Delta(2) + c_3 a_\Delta(3)) + a_\Delta(RC), \quad (44)$$

where the first term comes from  $V_{\text{TRV}}^{(3\pi,0)}$ , the term in parenthesis from  $V_{\text{TRV}}^{(3\pi,1)}$ , where the LECs  $c_1$ ,  $c_2$  and  $c_3$  appear, and the last term from  $V_{\text{TRV}}^{(3\pi,RC)}$ . In Table III we report the values of the coefficients  $a_\Delta(i)$  evaluated using the N4LO PC potential for the various cut-off. We observe that, taking individually the coefficients which multiplies the LECs  $c_i$ , their correction to the NLO is between 13 – 23% which is in line with what we expect from the chiral expansion. However, using the values of  $c_i$  given in Table I the total correction of  $V_{\text{TRV}}^{(3\pi,1)}$  is about 66%, which is very large compared to what we expect adding a new order in the potential. Therefore, the value of  $a_\Delta$  is very sensitive to the  $V_{\text{TRV}}^{(3\pi,1)}$  component of the potential and on the choice of the values of the constant  $c_i$  and in particular of  $c_3$ . This is reflected also in

$\Lambda(\text{MeV})$	450	500	550
$a_\Delta(0)$	-0.872	-0.894	-0.894
$a_\Delta(1)$	0.117	0.120	0.120
$a_\Delta(2)$	-0.119	-0.119	-0.117
$a_\Delta(3)$	-0.209	-0.207	-0.203
$a_\Delta(RC)$	-0.042	-0.037	-0.032

TABLE III. Values of the various components of the deuteron coefficients  $a_\Delta$  as given in Eq. (44) in units of  $e$  fm evaluated using the N4LO PC potential for the three different choices of cutoff parameters  $\Lambda$ .

TRV pot.	$a_n(=a_p)$	$a_1$	$a_\Delta$	$A_3$	$A_4$
Ref. [47](NLO)	0.939	0.183	-0.748	0.006	-0.006
This work (NLO)	0.939	0.200	-0.893	—	—
This work (N2LO)	0.939	0.197	-0.341	0.013	-0.013

TABLE IV. Comparison of the coefficients  $a_1$ ,  $a_\Delta$ ,  $A_3$  and  $A_4$  for the deuteron with the result of Refs. [47]. To be notice that in this work we use  $e > 0$ . For this work we report the calculation up to NLO and N2LO.

the large error associated with this coefficient reported in Table II. On the other hand, the  $V_{TRV}^{(3\pi,RC)}$  contribution is about  $\sim 4\%$  as expected for a relativistic corrections. We notice also that the values of the coefficients for the three different cut-off are compatible within the error bars.

We now compare our results with the values reported in Ref. [47] where the Authors used the same TRV potential at NLO with a N2LO PC potential with three-body forces [53, 57]. In Table IV we compare our results obtained with our TRV potential up to NLO and N2LO with a cutoff  $\Lambda = 500$  MeV with the ones reported in Ref. [47].

In order to compare the values of the  $A_i$  coefficient we divide the reported values for  $\frac{2(\hbar c)^3}{\Lambda_\chi^2 f_\pi}$  which permits to connect the two potentials. As can be seen from Table IV, our values at NLO seem to be systematically larger compared to the values reported in Ref. [47]. Even if we use a different PC potential, the reason should be found in the different regularization function. However, from a qualitative point of view there is a substantial agreement with Ref. [47]. Similar agreement has been founded for  $a_1$  with the result reported in Refs. [19, 49, 50] while are smaller compare the results reported in Refs. [42, 48].

### B. $^3\text{H}$ and $^3\text{He}$ EDMs

In this section we report the results obtained for the EDM of the  $^3\text{H}$  and  $^3\text{He}$ . The wave functions of  $^3\text{H}$  and  $^3\text{He}$  have been obtained with the hyperspherical harmonics (HH) [58, 59] from the Hamiltonians N4LO/N2LO-500, N4LO/N2LO-450 and N4LO/N2LO-550 discussed

$^3\text{H}$				$^3\text{He}$		
$\Lambda(\text{MeV})$	450	500	550	450	500	550
$a_\Delta(0)$	-0.716	-0.751	-0.758	-0.716	-0.749	-0.755
$a_\Delta(1)$	0.093	0.098	0.099	0.093	0.098	0.099
$a_\Delta(2)$	-0.107	-0.110	-0.110	-0.106	-0.109	-0.109
$a_\Delta(3)$	-0.194	-0.198	-0.198	-0.192	-0.196	-0.196
$a_\Delta(RC)$	-0.048	-0.046	-0.042	-0.048	-0.044	-0.041
$a_\Delta(3N)$	-0.202	-0.190	-0.205	-0.193	-0.180	-0.196

TABLE V. Values of the various components of  $a_\Delta$  as given in Eq. (46) for  $^3\text{H}$  and  $^3\text{He}$  in units of  $e$  fm evaluated using the N4LO/N2LO PC potential for the three different choices of cutoff parameters  $\Lambda$ .

in Sec. IV. Moreover, we evaluated also the errors on the numerical coefficients due to the chiral expansion as,

$$(\delta a_i)^2 = (\delta a_i^{\text{PC}})^2 + (\delta a_i^{\text{TRV}})^2 + (\delta a_i^\psi)^2, \quad (45)$$

where  $\delta a_i^{\text{PC}}$  and  $\delta a_i^{\text{TRV}}$  are the same as in Eq. (42), while  $\delta a_i^\psi$  is the error associated to the numerical accuracy of the 3-body wave function which we estimated to be of the order of  $\sim 1\%$ . The calculated values of the numerical coefficients for the three choices of the cutoff with their associated errors are reported in Table VI.

The  $a_\Delta$  can be written as,

$$a_\Delta = a_\Delta(0) + (c_1 a_\Delta(1) + c_2 a_\Delta(2) + c_3 a_\Delta(3)) + a_\Delta(RC) + a_\Delta(3N), \quad (46)$$

where  $a_\Delta(0)$ ,  $a_\Delta(1)$ ,  $a_\Delta(2)$ ,  $a_\Delta(3)$  and  $a_\Delta(RC)$  are defined as in Eq. (44) while  $a_\Delta(3N)$  represents the TRV 3-body potential contribution. In Table V we report the values of the coefficients  $a_\Delta(i)$  evaluated using the N4LO/N2LO- $\Lambda$  PC potential for the various cut-off. The  $a_\Delta(3N)$  give a correction to  $a_\Delta(0)$  of the order of the  $\sim 25\%$ , which is in line with the chiral perturbation theory prediction because both the contributions appear at the same order. For completeness we report in Table VIII of Appendix D the convergence pattern of this contribution as function of the HH basis expansion. For both  $^3\text{H}$  and  $^3\text{He}$ , using the values of the  $c_i$  reported in Table I, we have found a correction to  $a_\Delta(0)$  due to  $V_{TRV}^{(3\pi,1)}$  of  $\sim 79\%$ , and of order  $\sim 6\%$  due to  $V_{TRV}^{(3\pi,RC)}$ . While the RC are in line with what we expect, the  $V_{TRV}^{(3\pi,1)}$  corrections have much more impact on the values of  $a_\Delta$  than predicted by the chiral perturbation theory. The large correction due to  $V_{TRV}^{(3\pi,1)}$  that appears at N2LO is also reflected in the large uncertainties associated with this coefficient. Again, the estimated uncertainties depends critically on the adopted values of  $c_1$ ,  $c_2$ , and  $c_3$  (see Table I).

The contribution of the TPE diagrams to  $a_0$  and  $a_2$  are of the order of  $\sim 45\%$  and  $\sim 40\%$  respectively which is larger than expected from the chiral convergence and they are due mainly to the box diagram in Fig. 1. On the



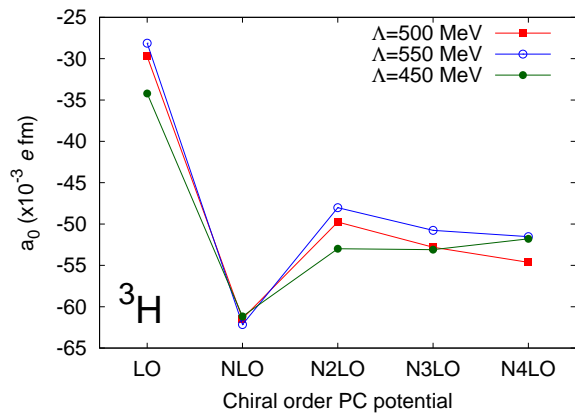


FIG. 2. Values of the coefficient  $a_0$  for the  $^3\text{H}$  nucleus and for the three choice of the cutoff when varying the chiral order of the PC potential.

other hand, the RC to  $a_0$ ,  $a_1$  and  $a_2$  are of the order of  $\sim 1 - 3\%$  perfectly consistent with the prediction of the chiral perturbation theory. The effects of the PC  $NNN$  potential on the values of all the coefficients is around  $\sim 2\%$ . From Table VI it is possible also to observe that the values of the numerical coefficients are mostly equal in modulus between  $^3\text{H}$  and  $^3\text{He}$  except  $a_p$  and  $a_n$ . Moreover, it is possible to observe that the isovector terms have the same sign for  $^3\text{H}$  and  $^3\text{He}$ . The isovector part of the TRV potential depends on the third component of the isospin, therefore the  $|\psi^A\rangle$  wave function component generated has a sign  $-$  for  $^3\text{H}$  and a  $+$  for  $^3\text{He}$ . However, in the  $\hat{D}_{\text{PC}}$  there is the  $\tau_z(i)$  operator which bring again a sign  $-$  for  $^3\text{H}$  and  $+$  for  $^3\text{He}$  giving in total a  $+$ .

In Table VII we compare our calculations at NLO for a value of the cutoff  $\Lambda = 500$  MeV with the values reported in Ref. [47]. As can be seen inspecting the values of the coefficients evaluated at NLO, there is a nice agreement with the results of Ref. [47]. The numerical

differences (which however are within the error bars reported in Ref. [47]) must be searched in the different PC potential and in the different regularization function in the TRV potential employed here. On the other hand for  $a_\Delta^{(3)}$ , the pure three body part of  $a_\Delta$ , the difference is of one order of magnitude which can not be explained by the different regularization function used. We found a good agreement for the values of  $a_0$  and  $a_1$  with the results obtained using a phenomenological potential and the meson exchange TRV potential in Refs. [49, 50] while we obtain smaller values compare to Refs. [42, 48].

In the case of  $^3\text{H}$  and  $^3\text{He}$  we studied also the dependence of the values of the coefficients on the chiral order of the PC potential. As example, in Fig. 2 and 3 we show the values of the coefficient  $a_0$  and  $a_\Delta^{(3)}$  for  $^3\text{H}$  evaluated using the N2LO TRV potential with different chiral order of the PC potential and for the three different choices of the cutoff. In all the case we studied, the values evaluated with the N2LO, N3LO and N4LO PC potential

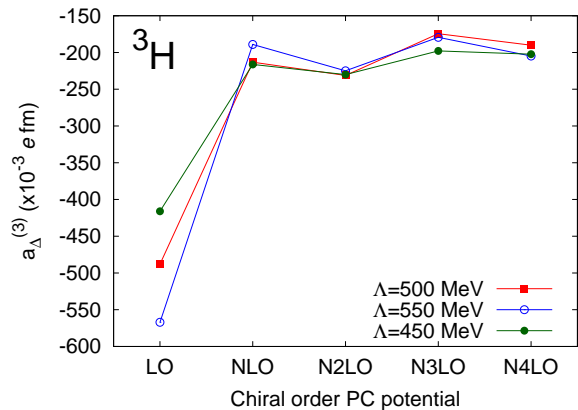


FIG. 3. The same as Fig. 2 but for the coefficient  $a_\Delta^{(3)}$ .

differ by less than 5% which confirm the robustness of the calculation.

## V. CONCLUSIONS

In this work we derived the TRV  $NN$  and  $NNN$  potential at N2LO. In order to derive the potential we have considered the most generic Lagrangian without any specific hypothesis for the TRV source. With the derived potential, we have calculated the EDM of  $^2\text{H}$ ,  $^3\text{H}$  and  $^3\text{He}$  investigating the effect of the N2LO components. We have found that the sensitivity of the light nuclei EDM to the LEC  $\Delta_3$  found at NLO, is well reduced by the N2LO contribution which is a quite unexpected behavior inside the chiral perturbation framework. We also checked the robustness of our calculation, evaluating the

EDM of the nuclei using different chiral orders in the PC potential. The discrepancy between the use of the N2LO and the N4LO PC potential is approximately 5%.

We have compared our results with the existing other values reported in literature and in particular with the calculation of Ref. [47]. We have found a substantial agreement with the results reported in Ref. [47] where the small numerical differences can be originated by the different function used to regularize the potential. We have found a qualitative agreement with those of Refs. [19, 49, 50] while we have obtained smaller values compared to Refs. [42, 48].

Our results depend on eleven coupling constants that

$\Lambda$ (MeV)	${}^3\text{H}$			${}^3\text{He}$		
	450	500	550	450	500	550
$a_n$	$-0.032 \pm 0.001$	$-0.033 \pm 0.001$	$-0.035 \pm 0.001$	$0.900 \pm 0.009$	$0.908 \pm 0.009$	$0.906 \pm 0.009$
$a_p$	$0.901 \pm 0.009$	$0.909 \pm 0.009$	$0.907 \pm 0.009$	$-0.032 \pm 0.001$	$-0.033 \pm 0.001$	$-0.034 \pm 0.001$
$a_0$	$-0.052 \pm 0.012$	$-0.055 \pm 0.013$	$-0.052 \pm 0.012$	$0.053 \pm 0.012$	$0.056 \pm 0.013$	$0.052 \pm 0.012$
$a_1$	$0.147 \pm 0.005$	$0.154 \pm 0.004$	$0.155 \pm 0.003$	$0.148 \pm 0.005$	$0.155 \pm 0.004$	$0.155 \pm 0.003$
$a_2$	$-0.114 \pm 0.010$	$-0.120 \pm 0.009$	$-0.121 \pm 0.008$	$0.112 \pm 0.009$	$0.118 \pm 0.009$	$0.119 \pm 0.008$
$a_\Delta$	$-0.378 \pm 0.105$	$-0.388 \pm 0.101$	$-0.407 \pm 0.088$	$-0.373 \pm 0.106$	$-0.383 \pm 0.102$	$-0.402 \pm 0.089$
$A_1$	$0.005 \pm 0.001$	$0.006 \pm 0.001$	$0.006 \pm 0.001$	$-0.005 \pm 0.002$	$-0.006 \pm 0.002$	$-0.006 \pm 0.001$
$A_2$	$-0.009 \pm 0.003$	$-0.010 \pm 0.003$	$-0.010 \pm 0.003$	$0.009 \pm 0.003$	$0.010 \pm 0.003$	$0.010 \pm 0.002$
$A_3$	$-0.008 \pm 0.002$	$-0.008 \pm 0.002$	$-0.008 \pm 0.002$	$-0.008 \pm 0.003$	$-0.008 \pm 0.002$	$-0.008 \pm 0.002$
$A_4$	$0.012 \pm 0.004$	$0.013 \pm 0.004$	$0.013 \pm 0.004$	$0.012 \pm 0.004$	$0.013 \pm 0.004$	$0.013 \pm 0.003$
$A_5$	$-0.021 \pm 0.006$	$-0.022 \pm 0.006$	$-0.022 \pm 0.006$	$0.020 \pm 0.006$	$0.022 \pm 0.006$	$0.022 \pm 0.005$

TABLE VI. Values of the numerical coefficients for  ${}^3\text{H}$  and  ${}^3\text{He}$  in units of  $e$  fm ( $a_n$  ( $a_p$ ) in units of  $d_n$  ( $d_p$ )) for the three different choices of the cutoff.

	${}^3\text{H}$			${}^3\text{He}$		
	This work	This work	Ref. [47]	This work	This work	Ref. [47]
	(NLO)	(N2LO)	(NLO)	(NLO)	(N2LO)	(NLO)
$a_n$	-0.033	-0.033	-0.030	0.908	0.908	0.904
$a_p$	0.909	0.909	0.918	-0.033	-0.033	-0.029
$a_0$	-0.101	-0.055	-0.108	0.101	0.056	0.111
$a_1$	0.158	0.154	0.139	0.158	0.155	0.139
$a_2$	0.087	0.120	n.a.	0.086	0.118	n.a.
$a_\Delta^{(2)}$	-0.751	-0.198	-0.598	-0.749	-0.202	-0.608
$a_\Delta^{(3)}$	-0.190	—	-0.017	-0.180	—	-0.017
$A_1$	—	0.006	0.005	—	-0.006	-0.005
$A_2$	—	-0.010	-0.011	—	0.010	0.011
$A_3$	—	-0.008	-0.005	—	-0.008	-0.005
$A_4$	—	0.013	0.009	—	0.013	0.009
$A_5$	—	-0.022	n.a.	—	0.022	n.a.

TABLE VII. Comparison of the values of the coefficients for  ${}^3\text{H}$  and  ${}^3\text{He}$  obtained for  $\Lambda = 500$  MeV with the results of Ref. [47].  $a_\Delta^{(2)}$  and  $a_\Delta^{(3)}$  correspond respectively to the 2-body and 3-body contribution to  $a_\Delta$ . To be noticed that in this work we use  $e > 0$ .

should be determined by comparing with experimental data. As many authors already pointed out [37, 38, 40], the size of the coupling constant depends on the CP violating model. Using our study it will be possible, in case of more than one measurements, to determine the LECs and then individuate the TRV source which generates the EDM by comparing the values of the calculated LECs and their predicted sizes.

In future, we plan to use  $\chi\text{EFT}$  to derive the TRV currents which give contribution at N2LO [45, 46]. This would allow to have a fully consistent calculation of the EDM of light nuclei up to N2LO. We also plan to study the  $\vec{n} - \vec{p}$  and  $\vec{n} - \vec{d}$  spin rotation for an independent and complementary study of TRV effects respect to EDM.

## ACKNOWLEDGMENTS

Computational resources provided by the INFN-Pisa Computer Center are gratefully acknowledged.

## Appendix A: Interaction vertices

It is convenient to decompose the interaction Hamiltonian  $H_I$  as follows

$$H_I = H^{00} + H^{01} + H^{10} + H^{02} + H^{11} + H^{20} + \dots, \quad (\text{A1})$$

where  $H^{nm}$  has  $n$  creation and  $m$  annihilation operators for the pion. Explicitly,

$$H^{00} = \frac{1}{\Omega} \sum_{\alpha'_1 \alpha_1 \alpha'_2 \alpha_2} b_{\alpha'_1}^\dagger b_{\alpha_1} b_{\alpha'_2}^\dagger b_{\alpha_2} M_{\alpha'_1 \alpha_1 \alpha'_2 \alpha_2}^{00} \delta_{\mathbf{p}'_1 + \mathbf{p}'_2, \mathbf{p}_1 + \mathbf{p}_2}, \quad (\text{A2})$$

$$H^{01} = \frac{1}{\sqrt{\Omega}} \sum_{\alpha' \alpha} \sum_{\mathbf{q} \mathbf{a}} b_{\alpha'}^\dagger b_{\alpha} a_{\mathbf{q} \mathbf{a}} M_{\alpha' \alpha, \mathbf{q} \mathbf{a}}^{01} \delta_{\mathbf{q} + \mathbf{p}, \mathbf{p}'}, \quad (\text{A3})$$

$$H^{10} = \frac{1}{\sqrt{\Omega}} \sum_{\alpha' \alpha} \sum_{\mathbf{q} \mathbf{a}} b_{\alpha'}^\dagger b_{\alpha} a_{\mathbf{q} \mathbf{a}}^\dagger M_{\alpha' \alpha, \mathbf{q} \mathbf{a}}^{10} \delta_{\mathbf{q} + \mathbf{p}', \mathbf{p}}, \quad (\text{A4})$$

$$H^{02} = \frac{1}{\Omega} \sum_{\alpha' \alpha} \sum_{\mathbf{q}' \mathbf{a}' \mathbf{q} \mathbf{a}} b_{\alpha'}^\dagger b_{\alpha} a_{\mathbf{q}' \mathbf{a}'} a_{\mathbf{q} \mathbf{a}} M_{\alpha' \alpha, \mathbf{q}' \mathbf{a}' \mathbf{q} \mathbf{a}}^{02} \delta_{\mathbf{q} + \mathbf{q}' + \mathbf{p}, \mathbf{p}'}, \quad (\text{A5})$$

$$H^{11} = \frac{1}{\Omega} \sum_{\alpha' \alpha} \sum_{\mathbf{q}' \mathbf{a}' \mathbf{q} \mathbf{a}} b_{\alpha'}^\dagger b_{\alpha} a_{\mathbf{q}' \mathbf{a}'}^\dagger a_{\mathbf{q} \mathbf{a}} M_{\alpha' \alpha, \mathbf{q}' \mathbf{a}' \mathbf{q} \mathbf{a}}^{11} \delta_{\mathbf{q} + \mathbf{p}, \mathbf{q}' + \mathbf{p}'}, \quad (\text{A6})$$

$$H^{20} = \frac{1}{\Omega} \sum_{\alpha' \alpha} \sum_{\mathbf{q}' \mathbf{a}' \mathbf{q} \mathbf{a}} b_{\alpha'}^\dagger b_{\alpha} a_{\mathbf{q}' \mathbf{a}'}^\dagger a_{\mathbf{q} \mathbf{a}}^\dagger M_{\alpha' \alpha, \mathbf{q}' \mathbf{a}' \mathbf{q} \mathbf{a}}^{20} \delta_{\mathbf{p}, \mathbf{q} + \mathbf{q}' + \mathbf{p}'}, \quad (\text{A7})$$

etc. Here  $\alpha_j \equiv \mathbf{p}_j, s_j, t_j$  denotes the momentum, spin projection, isospin projection of nucleon  $j$  with energy  $E_j = \sqrt{p_j^2 + M^2}$ ,  $\mathbf{q}$  and  $\mathbf{a}$  denote the momentum and isospin projection of a pion with energy  $\omega_q = \sqrt{q^2 + m_\pi^2}$ , and  $M^{nm}$  are the vertex functions listed below. The various momenta are discretized by assuming periodic boundary conditions in a box of volume  $\Omega$ . We note that in the expansion of the nucleon field  $\psi$  we have only retained the nucleon degrees of freedom, since anti-nucleon contributions do not enter the TRV  $NN$  and  $NNN$  potential at the order of interest here. We note also that in general the creation and annihilation operators are not normal-ordered. After normal-ordering them, tadpole-type contributions result, which are relevant only for renormalization, therefore we discard them hereafter.

The vertex functions  $M^{nm}$  involve products of Dirac 4-spinors, which are expanded non-relativistically in powers of momenta, and terms up to order  $Q^3$  are retained. Useful formulas are reported in Appendix F of Ref. [51].

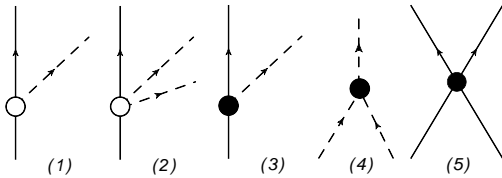


FIG. 4. Vertices entering the TRV potential at N2LO. The solid (dash) lines represent nucleons (pions). The open (solid) symbols denote PC (TRV) vertices.

The interaction vertices needed for the construction of the TRV potential, without considering renormalization contributions, are summarized in Fig. 4. Note that in the power counting of these vertices below, we do not include the  $1/\sqrt{\omega_k}$  normalization factors in the pion fields. We obtain:

1.  $\pi NN$  vertices. The PC interaction term is derived in Appendix F of Ref. [51]. For completeness, here we report the final formula for the PC vertex up to order  $Q^3$  that reads,

$$\begin{aligned} {}^{PC}M_{\alpha' \alpha, \mathbf{q} \mathbf{a}}^{\pi NN, 01} &= \frac{g_A}{2f_\pi} \frac{\tau_a}{\sqrt{2\omega_q}} \left[ i \mathbf{q} \cdot \boldsymbol{\sigma} - \frac{i}{M} \omega_q \mathbf{K} \cdot \boldsymbol{\sigma} \right. \\ &\quad \left. + \frac{i}{4M^2} (2\mathbf{K} \cdot \mathbf{q} \mathbf{K} \cdot \boldsymbol{\sigma} - 2K^2 \mathbf{q} \cdot \boldsymbol{\sigma} - \frac{1}{2} \mathbf{k} \cdot \boldsymbol{\sigma} \mathbf{q} \cdot \mathbf{k}) \right] \\ &\quad + \frac{m_\pi^2}{f_\pi} (2d_{16} - d_{18}) \frac{\tau_a}{\sqrt{2\omega_q}} i \mathbf{q} \cdot \boldsymbol{\sigma}, \quad (\text{A8}) \end{aligned}$$

$${}^{PC}M_{\alpha' \alpha, \mathbf{q} \mathbf{a}}^{\pi NN, 10} = - {}^{PC}M_{\alpha' \alpha, \mathbf{q} \mathbf{a}}^{\pi NN, 01}. \quad (\text{A9})$$

In diagrams, these PC vertex functions are represented as open circles. The TRV  $\pi NN$  vertices are due to interaction terms proportional to LECs  $g_0$ ,  $g_1$  and  $g_2$  which corresponds to isoscalar, isovector and isotensor interaction, plus terms which derive from  $\mathcal{L}_{\text{TRV}}^{\pi N (1)}$  and  $\mathcal{L}_{\text{TRV}}^{\pi N (2)}$  given in Eqs. (3) and (4). They read (up to order  $Q^2$ ),

$$\begin{aligned} {}^{TRV}M_{\alpha' \alpha, \mathbf{q} \mathbf{a}}^{\pi NN, 01} &= - \frac{(g_0 \tau_a + g_1 \delta_{a,3} + g_2 \tau_3 \delta_{a,3})}{\sqrt{2\omega_q}} \\ &\quad \times \left[ 1 - \frac{1}{4M^2} (2K^2 + i \mathbf{k} \times \mathbf{K}) \right] \\ &\quad - i g_V^{(1)} \frac{\epsilon_{ab3} \tau_b}{f_\pi \sqrt{2\omega_q}} \left[ \omega_q - \frac{1}{2M} \mathbf{K} \cdot \mathbf{q} \right] \\ &\quad + \frac{m_\pi^2}{f_\pi^2 \sqrt{2\omega_q}} (g_{S1}^{(2)} \tau_a + g_{V1}^{(2)} \delta_{a,3} + g_{T1}^{(2)} \tau_3 \delta_{a,3}) \\ &\quad - \frac{\omega_q^2}{f_\pi^2 \sqrt{2\omega_q}} (g_{S2}^{(2)} \tau_a + g_{V2}^{(2)} \delta_{a,3} + g_{T2}^{(2)} \tau_3 \delta_{a,3}), \quad (\text{A10}) \end{aligned}$$

$$\begin{aligned} {}^{TRV}M_{\alpha' \alpha, \mathbf{q} \mathbf{a}}^{\pi NN, 10} &= - \frac{(g_0 \tau_a + g_1 \delta_{a,3} + g_2 \tau_3 \delta_{a,3})}{\sqrt{2\omega_q}} \\ &\quad \times \left[ 1 - \frac{1}{4M^2} (2K^2 + i \mathbf{k} \times \mathbf{K}) \right] \\ &\quad + i g_V^{(1)} \frac{\epsilon_{ab3} \tau_b}{f_\pi \sqrt{2\omega_q}} \left[ \omega_q - \frac{1}{2M} \mathbf{K} \cdot \mathbf{q} \right] \\ &\quad + \frac{m_\pi^2}{f_\pi^2 \sqrt{2\omega_q}} (g_{S1}^{(2)} \tau_a + g_{V1}^{(2)} \delta_{a,3} + g_{T1}^{(2)} \tau_3 \delta_{a,3}) \\ &\quad - \frac{\omega_q^2}{f_\pi^2 \sqrt{2\omega_q}} (g_{S2}^{(2)} \tau_a + g_{V2}^{(2)} \delta_{a,3} + g_{T2}^{(2)} \tau_3 \delta_{a,3}), \quad (\text{A11}) \end{aligned}$$

2.  $\pi\pi NN$  vertices. The PC interaction is needed up to NLO in the NR expansion at the order we are interested. The corresponding vertex functions will receive contribution from the Weinberg-Tomozawa term and from  $\mathcal{L}_{N\pi}^{(2)}$ . The vertex functions read,

$$\begin{aligned} {}^{PC}M_{\alpha'\alpha, \mathbf{q}'a' \mathbf{q}a}^{\pi\pi NN, 02} &= \frac{i}{8f_\pi^2} \frac{\epsilon_{aa'b}\tau_b}{\sqrt{2\omega_q}\sqrt{2\omega_{q'}}} \left[ (\omega_q - \omega_{q'}) \right. \\ &\quad \left. - \frac{2\mathbf{K} \cdot (\mathbf{q} - \mathbf{q}') - i(\mathbf{k} \times \boldsymbol{\sigma}) \cdot (\mathbf{q} - \mathbf{q}')}{2M} \right] \\ &\quad + \frac{\delta_{ij}}{f_\pi^2} \frac{c_1(2m_\pi^2) + c_2\omega_q\omega_{q'} + c_3(\omega_q\omega_{q'} - \mathbf{q} \cdot \mathbf{q}')}{\sqrt{2\omega_q}\sqrt{2\omega_{q'}}} \\ &\quad - \frac{c_4}{2f_\pi^2} \frac{\epsilon_{aa'b}\tau_b}{\sqrt{2\omega_q}\sqrt{2\omega_{q'}}} (\mathbf{q} \times \mathbf{q}') \cdot \boldsymbol{\sigma}, \end{aligned} \quad (\text{A12})$$

$$\begin{aligned} {}^{PC}M_{\alpha'\alpha, \mathbf{q}'a' \mathbf{q}a}^{\pi\pi NN, 20} &= \frac{i}{8f_\pi^2} \frac{\epsilon_{aa'b}\tau_b}{\sqrt{2\omega_q}\sqrt{2\omega_{q'}}} \left[ (\omega_{q'} - \omega_q) \right. \\ &\quad \left. - \frac{2\mathbf{K} \cdot (\mathbf{q}' - \mathbf{q}) - i(\mathbf{k} \times \boldsymbol{\sigma}) \cdot (\mathbf{q}' - \mathbf{q})}{2M} \right] \\ &\quad + \frac{\delta_{ij}}{f_\pi^2} \frac{c_1(2m_\pi^2) + c_2\omega_q\omega_{q'} + c_3(\omega_q\omega_{q'} - \mathbf{q} \cdot \mathbf{q}')}{\sqrt{2\omega_q}\sqrt{2\omega_{q'}}} \\ &\quad - \frac{c_4}{2f_\pi^2} \frac{\epsilon_{aa'b}\tau_b}{\sqrt{2\omega_q}\sqrt{2\omega_{q'}}} (\mathbf{q} \times \mathbf{q}') \cdot \boldsymbol{\sigma}. \end{aligned} \quad (\text{A13})$$

The  ${}^{PC}M_{\alpha'\alpha, \mathbf{q}'a' \mathbf{q}a}^{\pi\pi NN, 11}$  vertex is not needed for the evaluation of the time-ordered diagrams.

3.  $3\pi$  vertices. The TRV Lagrangian has a three-pion interaction term shown in diagram (4) of Fig. 4. The vertices, neglecting the tadpole terms, are given by  $H_I^{3\pi} = H_I^{3\pi, 03} + H_I^{3\pi, 12} + H_I^{3\pi, 21} + H_I^{3\pi, 30}$ , where

$$H_I^{3\pi, 03} = \frac{1}{\Omega^{3/2}} \sum_{\mathbf{q}a \mathbf{q}'a' \mathbf{p}b} a_{\mathbf{q}a} a_{\mathbf{q}'a'} a_{\mathbf{p}b} M_{\mathbf{q}a \mathbf{q}'a' \mathbf{p}b}^{3\pi, 03} \delta_{\mathbf{q}+\mathbf{q}'+\mathbf{p}, 0}, \quad (\text{A14})$$

$$H_I^{3\pi, 12} = \frac{1}{\Omega^{3/2}} \sum_{\mathbf{q}a \mathbf{q}'a' \mathbf{p}b} a_{\mathbf{q}a} a_{\mathbf{q}'a'} a_{\mathbf{p}b}^\dagger M_{\mathbf{q}a \mathbf{q}'a' \mathbf{p}b}^{3\pi, 12} \delta_{\mathbf{q}+\mathbf{q}', \mathbf{p}}, \quad (\text{A15})$$

$$H_I^{3\pi, 21} = \frac{1}{\Omega^{3/2}} \sum_{\mathbf{q}a \mathbf{q}'a' \mathbf{p}b} a_{\mathbf{q}a} a_{\mathbf{q}'a'}^\dagger a_{\mathbf{p}b}^\dagger M_{\mathbf{q}a \mathbf{q}'a' \mathbf{p}b}^{3\pi, 21} \delta_{\mathbf{q}, \mathbf{q}'+\mathbf{p}}, \quad (\text{A16})$$

$$H_I^{3\pi, 30} = \frac{1}{\Omega^{3/2}} \sum_{\mathbf{q}a \mathbf{q}'a' \mathbf{p}b} a_{\mathbf{q}a}^\dagger a_{\mathbf{q}'a'}^\dagger a_{\mathbf{p}b}^\dagger M_{\mathbf{q}a \mathbf{q}'a' \mathbf{p}b}^{3\pi, 30} \delta_{0, \mathbf{q}+\mathbf{q}'+\mathbf{p}}, \quad (\text{A17})$$

with,

$$\begin{aligned} {}^{TRV}M_{\mathbf{q}a \mathbf{q}'a' \mathbf{p}b}^{3\pi, 03} &= -\frac{\Delta M}{3\sqrt{2\omega_q} 2\omega_{q'} 2\omega_p} \\ &\quad \times (\delta_{a,a'}\delta_{b,3} + \delta_{a,b}\delta_{a',3} + \delta_{a',b}\delta_{a,3}), \end{aligned}$$

$$(\text{A18})$$

$${}^{TRV}M_{\mathbf{q}a \mathbf{q}'a' \mathbf{p}b}^{3\pi, 12} = 3 {}^{TRV}M_{\mathbf{q}a \mathbf{q}'a' \mathbf{p}b}^{3\pi, 03}, \quad (\text{A19})$$

$${}^{TRV}M_{\mathbf{q}a \mathbf{q}'a' \mathbf{p}b}^{3\pi, 21} = 3 {}^{TRV}M_{\mathbf{q}a \mathbf{q}'a' \mathbf{p}b}^{3\pi, 03}, \quad (\text{A20})$$

$${}^{TRV}M_{\mathbf{q}a \mathbf{q}'a' \mathbf{p}b}^{3\pi, 30} = {}^{TRV}M_{\mathbf{q}a \mathbf{q}'a' \mathbf{p}b}^{3\pi, 03}. \quad (\text{A21})$$

4.  $4N$  contact interaction. The EFT Hamiltonian includes also the term given in Eq. (A2) derived from a contact Lagrangian. We only need its TRV part of order  $Q$ , which includes five independent interaction terms. With a suitable choice of the LECs, the vertex function  ${}^{TRV}M^{00}$  can be written as

$$\begin{aligned} {}^{TRV}M_{\alpha'_1\alpha_1\alpha'_2\alpha_2}^{00} &= \frac{1}{2\Lambda_\chi^2 f_\pi} \left[ C_1 i\mathbf{k}_1 \cdot (\boldsymbol{\sigma}_1 - \boldsymbol{\sigma}_2) \right. \\ &\quad + C_2 \boldsymbol{\tau}_1 \cdot \boldsymbol{\tau}_2 i\mathbf{k}_1 \cdot (\boldsymbol{\sigma}_1 - \boldsymbol{\sigma}_2) \\ &\quad + \frac{C_3}{2} ((\tau_{1z} + \tau_{2z}) i\mathbf{k}_1 \cdot (\boldsymbol{\sigma}_1 - \boldsymbol{\sigma}_2) \\ &\quad \quad - (\tau_{1z} - \tau_{2z}) i\mathbf{k}_1 \cdot (\boldsymbol{\sigma}_1 + \boldsymbol{\sigma}_2)) \\ &\quad + \frac{C_4}{2} ((\tau_{1z} + \tau_{2z}) i\mathbf{k}_1 \cdot (\boldsymbol{\sigma}_1 - \boldsymbol{\sigma}_2) \\ &\quad \quad + (\tau_{1z} - \tau_{2z}) i\mathbf{k}_1 \cdot (\boldsymbol{\sigma}_1 + \boldsymbol{\sigma}_2)) \\ &\quad \left. + C_5 (3\tau_{1z}\tau_{2z} - \boldsymbol{\tau}_1 \cdot \boldsymbol{\tau}_2) i\mathbf{k}_1 \cdot (\boldsymbol{\sigma}_1 - \boldsymbol{\sigma}_2) \right], \end{aligned} \quad (\text{A22})$$

where  $\mathbf{k}_1 = \mathbf{p}'_1 - \mathbf{p}_1 = -\mathbf{p}'_2 + \mathbf{p}_2$ .

## Appendix B: The TRV $NN$ potential

In this section we discuss the derivation of the TRV  $NN$  and  $NNN$  potential, providing explicit expressions of the diagrams given in Fig. 1. The power counting is as follows: (i) a PC (TRV)  $\pi NN$  vertex is of order  $Q$  ( $Q^0$ ); (ii) a PC  $\pi\pi NN$  vertex is of order  $Q^1$ ; (iii) a TRV  $3\pi$  vertex is of order  $Q^{-3}$ ; (iv) a PC (TRV)  $NN$  contact vertex is of order  $Q^0$  ( $Q$ ); (v) an energy denominator without (with one or more) pions is of order  $Q^{-2}$  ( $Q^{-1}$ ); (vi) factors  $Q^{-1}$  and  $Q^3$  are associated with, respectively, each pion line and each loop integration. The momenta are defined as given in Eq. (21), and in what follows use is made of the fact that  $\mathbf{k} \cdot \mathbf{K}$  vanishes in the c.m. frame. It is useful to define the isospin operator as,

$$T_0 = \boldsymbol{\tau}_1 \cdot \boldsymbol{\tau}_2, \quad (\text{B1})$$

$$T_1^+ = (\tau_{1z} + \tau_{2z}), \quad (\text{B2})$$

$$T_1^- = (\tau_{1z} - \tau_{2z}), \quad (\text{B3})$$

$$T_2 = (3\tau_{1z}\tau_{2z} - \boldsymbol{\tau}_1 \cdot \boldsymbol{\tau}_2). \quad (\text{B4})$$

The TRV  $NN$  potential is derived from the amplitudes in Fig. 1 via Eqs. (18)–(20). Up to order  $Q$  included, we obtain for the OPE component in panel (a) of Fig. 1 :

$$V(a) = V^{(-1)}(\text{NR}) + V^{(1)}(\text{RC}) + V^{(1)}(\text{LEC}), \quad (\text{B5})$$



where,

$$V^{(-1)}(\text{NR}) = \frac{g_A g_0^*}{2f_\pi} T_0 \frac{i\mathbf{k} \cdot (\boldsymbol{\sigma}_1 - \boldsymbol{\sigma}_2)}{\omega_k^2} + \frac{g_A g_1}{4f_\pi} \left[ T_1^+ \frac{i\mathbf{k} \cdot (\boldsymbol{\sigma}_1 - \boldsymbol{\sigma}_2)}{\omega_k^2} + T_1^- \frac{i\mathbf{k} \cdot (\boldsymbol{\sigma}_1 + \boldsymbol{\sigma}_2)}{\omega_k^2} \right] + \frac{g_A g_2}{6f_\pi} T_2 \frac{i\mathbf{k} \cdot (\boldsymbol{\sigma}_1 - \boldsymbol{\sigma}_2)}{\omega_k^2}, \quad (\text{B6})$$

$$V_{TRV}^{(1)}(\text{RC}) = \frac{g_A g_0^*}{8f_\pi M^2} T_0 \frac{1}{\omega_k^2} \times \left[ -\frac{i}{2} (8K^2 + k^2) \mathbf{k} \cdot (\boldsymbol{\sigma}_1 - \boldsymbol{\sigma}_2) + \mathbf{k} \cdot \boldsymbol{\sigma}_1 (\mathbf{k} \times \mathbf{K}) \cdot \boldsymbol{\sigma}_2 - \mathbf{k} \cdot \boldsymbol{\sigma}_2 (\mathbf{k} \times \mathbf{K}) \cdot \boldsymbol{\sigma}_1 \right] + \frac{g_A g_1}{16f_\pi M^2} \frac{1}{\omega_k^2} \times \left\{ T_1^- \left[ -\frac{i}{2} (8K^2 + k^2) \mathbf{k} \cdot (\boldsymbol{\sigma}_1 + \boldsymbol{\sigma}_2) + \mathbf{k} \cdot \boldsymbol{\sigma}_1 (\mathbf{k} \times \mathbf{K}) \cdot \boldsymbol{\sigma}_2 + \mathbf{k} \cdot \boldsymbol{\sigma}_2 (\mathbf{k} \times \mathbf{K}) \cdot \boldsymbol{\sigma}_1 \right] + T_1^+ \left[ -\frac{i}{2} (8K^2 + k^2) \mathbf{k} \cdot (\boldsymbol{\sigma}_1 - \boldsymbol{\sigma}_2) + \mathbf{k} \cdot \boldsymbol{\sigma}_1 (\mathbf{k} \times \mathbf{K}) \cdot \boldsymbol{\sigma}_2 - \mathbf{k} \cdot \boldsymbol{\sigma}_2 (\mathbf{k} \times \mathbf{K}) \cdot \boldsymbol{\sigma}_1 \right] \right\} + \frac{g_A g_2}{24f_\pi M^2} T_2 \frac{1}{\omega_k^2} \left[ -\frac{i}{2} (8K^2 + k^2) \mathbf{k} \cdot (\boldsymbol{\sigma}_1 - \boldsymbol{\sigma}_2) + \mathbf{k} \cdot \boldsymbol{\sigma}_1 (\mathbf{k} \times \mathbf{K}) \cdot \boldsymbol{\sigma}_2 - \mathbf{k} \cdot \boldsymbol{\sigma}_2 (\mathbf{k} \times \mathbf{K}) \cdot \boldsymbol{\sigma}_1 \right], \quad (\text{B7})$$

$$V_{TRV}^{(1)}(\text{LEC}) = V_{TRV}^{(-1)}(\text{NR}) \frac{2m_\pi^2}{g_A} (2d_{16} - d_{18}) + \frac{g_A}{2f_\pi^3} T_0 i\mathbf{k} \cdot (\boldsymbol{\sigma}_1 - \boldsymbol{\sigma}_2) \left[ g_{S2}^{(2)} - g_{S1}^{(2)} \frac{m_\pi^2}{\omega_k^2} \right] + \frac{g_A}{4f_\pi^3} \left[ T_1^+ i\mathbf{k} \cdot (\boldsymbol{\sigma}_1 - \boldsymbol{\sigma}_2) + T_1^- i\mathbf{k} \cdot (\boldsymbol{\sigma}_1 + \boldsymbol{\sigma}_2) \right] \times \left[ g_{V2}^{(2)} - g_{V1}^{(2)} \frac{m_\pi^2}{\omega_k^2} \right] + \frac{g_A}{6f_\pi^3} T_2 i\mathbf{k} \cdot (\boldsymbol{\sigma}_1 - \boldsymbol{\sigma}_2) \left[ g_{T2}^{(2)} - g_{T1}^{(2)} \frac{m_\pi^2}{\omega_k^2} \right] + \frac{g_V^{(1)} g_A}{2f_\pi^2 M} (\boldsymbol{\tau}_1 \times \boldsymbol{\tau}_2)_z \mathbf{K} \cdot (\boldsymbol{\sigma}_1 + \boldsymbol{\sigma}_2), \quad (\text{B8})$$

where  $g_0^* = g_0 + g_2/3$ . The contribution given in the first line of Eq. (B8) renormalizes the coupling constants  $g_0^*$ ,  $g_1$  and  $g_2$  in the OPE term. The terms of Eq. (B8) which are multiplied by the factor  $m_\pi^2/\omega_k^2$  are also reabsorbed in the constant  $g_0^*$ ,  $g_1$  and  $g_2$  while all the other terms are reabsorbed in the LECs  $C_2$ ,  $C_4$  and  $C_5$  in Eq. (30). Regarding the last term in Eq. (B8), it is possible to use a Fierz transformation obtaining a combination of the operators which multiplies the LECs  $C_3$  and  $C_4$ . Therefore all  $V_{TRV}^{(1)}(\text{LEC})$  can be reabsorbed in the OPE and contact potentials. The factor  $k^2 = \omega_k^2 - m_\pi^2$  in the isoscalar,

isovector and isotensor component of  $V^{(1)}(\text{RC})$  leads to a piece that can be reabsorbed in the contact term proportional to  $C_2$ ,  $C_4$  and  $C_5$  in Eq. (30) and a piece proportional to  $m_\pi^2$  that simply renormalizes the LECs  $g_0^*$ ,  $g_1$  and  $g_2$ .

The component of the TRV potential coming from the contact terms in panel (b) of Fig. 1 derives directly from the vertex function  $^{TRV}M^{00}$  given in Eq. (A22). The final expression has already been given in Eq. (30). The diagrams reported in panels (c) and (d) contain a combination of a contact interaction with the exchange of a pion. However, it can be shown that their contribution is at least of order  $Q^3$ .

Next we consider the TPE components in panels (e)-(h). The contribution from diagrams (e) reads,

$$V^{(1)}(\text{e}) = -\frac{g_A g_0^*}{4f_\pi^3} T_0 i\mathbf{k} \cdot (\boldsymbol{\sigma}_1 - \boldsymbol{\sigma}_2) \int_{\mathbf{q}} \frac{1}{\omega_+ \omega_- (\omega_+ + \omega_-)} + \frac{g_A g_2}{12f_\pi^3} T_2 i\mathbf{k} \cdot (\boldsymbol{\sigma}_1 - \boldsymbol{\sigma}_2) \int_{\mathbf{q}} \frac{1}{\omega_+ \omega_- (\omega_+ + \omega_-)}, \quad (\text{B9})$$

where  $\omega_\pm = \sqrt{(\mathbf{k} \pm \mathbf{q})^2 + 4m_\pi^2}$  and  $\int_{\mathbf{q}} = \int \frac{d\mathbf{q}}{(2\pi)^3}$ . The isovector component of the OPE vertex vanishes since the integrand is proportional to  $\mathbf{q}$ , therefore there is no isovector component from panel (e). Dimensional regularization allows one to obtain the finite part as,

$$\bar{V}^{(1)}(\text{e}) = \frac{g_A g_0^*}{f_\pi \Lambda_\chi^2} T_0 i\mathbf{k} \cdot (\boldsymbol{\sigma}_1 - \boldsymbol{\sigma}_2) L(k) - \frac{g_A g_2}{3f_\pi \Lambda_\chi^2} T_2 i\mathbf{k} \cdot (\boldsymbol{\sigma}_1 - \boldsymbol{\sigma}_2) L(k), \quad (\text{B10})$$

where  $\Lambda_\chi = 4\pi f_\pi$  and the loop function  $L(k)$  is defined as

$$L(k) = \frac{1}{2} \frac{s}{k} \ln \left( \frac{s+k}{s-k} \right), \quad s = \sqrt{k^2 + 4m_\pi^2}. \quad (\text{B11})$$

The singular part is given by,

$$V_\infty^{(1)}(\text{e}) = \frac{g_A g_0^*}{2f_\pi \Lambda_\chi^2} T_0 i\mathbf{k} \cdot (\boldsymbol{\sigma}_1 - \boldsymbol{\sigma}_2) (d_\epsilon - 2) - \frac{g_A g_2}{6f_\pi \Lambda_\chi^2} T_2 i\mathbf{k} \cdot (\boldsymbol{\sigma}_1 - \boldsymbol{\sigma}_2) (d_\epsilon - 2), \quad (\text{B12})$$

where

$$d_\epsilon = -\frac{2}{\epsilon} + \gamma - \ln \pi + \ln \left( \frac{m_\pi^2}{\mu^2} \right), \quad (\text{B13})$$

$\epsilon = 3 - d$ ,  $d$  being the number of dimensions ( $d \rightarrow 3$ ), and  $\mu$  is a renormalization scale. This singular contribution is absorbed in the  $V_{TRV}^{(\text{CT})}$  term proportional to  $C_2$  for the isoscalar part and to  $C_5$  for the isotensor part.

The contributions from panels (f)-(h) in Fig. 1 are collectively denoted as “box” below, and the non-iterative pieces in reducible diagrams of type (h) are identified via Eq. (20). From the panel (f) we obtain,

$$V^{(1)}(\text{f}) = \left\{ -\frac{g_A^3 g_0^*}{16f_\pi^3} (3 + 2 T_0) i\mathbf{k} \cdot (\boldsymbol{\sigma}_1 - \boldsymbol{\sigma}_2) \right.$$

$$\begin{aligned}
& + \frac{g_A^3 g_2}{48 f_\pi^3} T_2 \, i\mathbf{k} \cdot (\boldsymbol{\sigma}_1 - \boldsymbol{\sigma}_2) \\
& - \frac{g_A^3 g_1}{32 f_\pi^3} \left[ T_1^+ i\mathbf{k} \cdot (\boldsymbol{\sigma}_1 - \boldsymbol{\sigma}_2) + T_1^- i\mathbf{k} \cdot (\boldsymbol{\sigma}_1 + \boldsymbol{\sigma}_2) \right] \Big\} \\
& \times \int_{\mathbf{q}} \frac{\omega_+^2 + \omega_+ \omega_- + \omega_-^2}{\omega_+^3 \omega_-^3 (\omega_+ + \omega_-)} (k^2 - q^2), \quad (B14)
\end{aligned}$$

while the contribution of panel (g) results,

$$\begin{aligned}
V^{(1)}(g) = & \left\{ \frac{g_A^3 g_0^*}{16 f_\pi^3} (3 - 2 T_0) i\mathbf{k} \cdot (\boldsymbol{\sigma}_1 - \boldsymbol{\sigma}_2) \right. \\
& + \frac{g_A^3 g_2}{48 f_\pi^3} T_2 \, i\mathbf{k} \cdot (\boldsymbol{\sigma}_1 - \boldsymbol{\sigma}_2) \\
& + \frac{g_A^3 g_1}{32 f_\pi^3} \left[ T_1^+ i\mathbf{k} \cdot (\boldsymbol{\sigma}_1 - \boldsymbol{\sigma}_2) + T_1^- i\mathbf{k} \cdot (\boldsymbol{\sigma}_1 + \boldsymbol{\sigma}_2) \right] \Big\} \\
& \times \int_{\mathbf{q}} \frac{\omega_+^2 + \omega_+ \omega_- + \omega_-^2}{\omega_+^3 \omega_-^3 (\omega_+ + \omega_-)} (k^2 - q^2). \quad (B15)
\end{aligned}$$

The complete “box” contribution is given by the sum of  $V(f)$  and  $V(g)$  and it reads,

$$\begin{aligned}
V^{(1)}(\text{box}) = & \left\{ - \frac{g_A^3 g_0^*}{4 f_\pi^3} T_0 \, i\mathbf{k} \cdot (\boldsymbol{\sigma}_1 - \boldsymbol{\sigma}_2) \right. \\
& + \frac{g_A^3 g_2}{12 f_\pi^3} T_2 \, i\mathbf{k} \cdot (\boldsymbol{\sigma}_1 - \boldsymbol{\sigma}_2) \Big\} \\
& \times \int_{\mathbf{q}} \frac{\omega_+^2 + \omega_+ \omega_- + \omega_-^2}{\omega_+^3 \omega_-^3 (\omega_+ + \omega_-)} (k^2 - q^2), \quad (B16)
\end{aligned}$$

where all the isovector terms cancel out. After dimensional regularization, the finite part reads,

$$\begin{aligned}
\bar{V}^{(1)}(\text{box}) = & \frac{g_A^3 g_0^*}{f_\pi \Lambda_\chi^2} T_0 \, i\mathbf{k} \cdot (\boldsymbol{\sigma}_1 - \boldsymbol{\sigma}_2) [H(k) - 3 L(k)] \\
& - \frac{g_A^3 g_2}{3 f_\pi \Lambda_\chi^2} T_2 \, i\mathbf{k} \cdot (\boldsymbol{\sigma}_1 - \boldsymbol{\sigma}_2) [H(k) - 3 L(k)], \quad (B17)
\end{aligned}$$

where

$$H(k) = \frac{4 m_\pi^2}{s^2} L(k), \quad (B18)$$

while the singular part is given by,

$$\begin{aligned}
V_\infty^{(1)}(\text{box}) = & - \frac{g_A^3 g_0^*}{f_\pi \Lambda_\chi^2} T_0 \, i\mathbf{k} \cdot (\boldsymbol{\sigma}_1 - \boldsymbol{\sigma}_2) \left( \frac{3}{2} d_\epsilon - 1 \right) \\
& + \frac{g_A^3 g_2}{3 f_\pi \Lambda_\chi^2} T_2 \, i\mathbf{k} \cdot (\boldsymbol{\sigma}_1 - \boldsymbol{\sigma}_2) \left( \frac{3}{2} d_\epsilon - 1 \right). \quad (B19)
\end{aligned}$$

The latter is absorbed in the  $V_{TRV}^{(\text{CT})}$  term proportional to  $C_2$  for the isoscalar part and to  $C_5$  for the isotensor part.

Now we consider the contributions that come from the panels (i) and (l) of Fig. 1. At NLO the contributions of the panel (l) cancel out due to the isospin structure of the vertices. The contribution of diagrams (i) result,

$$V^{(0)}(i) = - \frac{5 g_A^3 \Delta_3 M}{32 f_\pi^3} \frac{1}{\omega_k^2} \left[ T_1^+ i\mathbf{k} \cdot (\boldsymbol{\sigma}_1 - \boldsymbol{\sigma}_2) \right.$$

$$\left. + T_1^- i\mathbf{k} \cdot (\boldsymbol{\sigma}_1 + \boldsymbol{\sigma}_2) \right] \int_{\mathbf{q}} \frac{k^2 - q^2}{\omega_+^2 \omega_-^2}. \quad (B20)$$

Using dimensional regularization we obtain,

$$\begin{aligned}
\bar{V}^{(0)}(i) = & - \frac{5 g_A^3 \Delta_3 M}{4 f_\pi \Lambda_\chi^2} \frac{\pi}{\omega_k^2} (T_1^- i\mathbf{k} \cdot (\boldsymbol{\sigma}_1 - \boldsymbol{\sigma}_2) \\
& + T_1^+ i\mathbf{k} \cdot (\boldsymbol{\sigma}_1 - \boldsymbol{\sigma}_2)) \left[ \left( 1 - \frac{2 m_\pi^2}{s^2} \right) s^2 A(k) + m_\pi \right], \quad (B21)
\end{aligned}$$

where,

$$A(k) = \frac{1}{2k} \arctan \left( \frac{k}{2m_\pi} \right). \quad (B22)$$

To be noticed that the use of dimensional regularization does not give the divergent part of the integral in Eq. (B20). This is due to the fact that the dimensional regularization cannot deal with linear divergences. To explicit the linear divergence we use a simple regularization of Eq. (B20), namely we integrate over  $q$  up to a (large) value  $\Lambda_R$ . The result for the non divergent part is equal to the one reported in Eq. (B20) while the divergent part reads,

$$\begin{aligned}
V_\infty^{(0)}(i) = & - \frac{5 g_A^3 \Delta_3 M}{4 f_\pi \Lambda_\chi^2} \frac{1}{\omega_k^2} (T_1^- i\mathbf{k} \cdot (\boldsymbol{\sigma}_1 - \boldsymbol{\sigma}_2) \\
& + T_1^+ i\mathbf{k} \cdot (\boldsymbol{\sigma}_1 - \boldsymbol{\sigma}_2)) \left[ \Lambda_R + \mathcal{O}\left(\frac{k^2}{\Lambda_R}\right) \right], \quad (B23)
\end{aligned}$$

where spurious contributions of order  $Q^2/\Lambda_R$  or more appear but they can be neglected for  $\Lambda_R \rightarrow \infty$ . The divergent part can be reabsorbed in the  $V_{TRV}^{(\text{CT})}$  term proportional to  $C_4$ .

At N2LO the contribution of panel (i) comes both from the second order in the pion propagator (PP) and in the pion-nucleon vertex (PNV). For the former we obtain,

$$\begin{aligned}
V^{(1)}(i - \text{PP}) = & - \frac{5 g_A^3 \Delta_3}{128 f_\pi^3} \frac{1}{\omega_k^2} \left[ T_1^+ i\mathbf{k} \cdot (\boldsymbol{\sigma}_1 - \boldsymbol{\sigma}_2) \right. \\
& + T_1^- i\mathbf{k} \cdot (\boldsymbol{\sigma}_1 + \boldsymbol{\sigma}_2) \Big] \int_{\mathbf{q}} \frac{\omega_+^2 + \omega_+ \omega_- + \omega_-^2}{\omega_+^3 \omega_-^3 (\omega_+ + \omega_-)} (k^2 - q^2)^2 \\
& + \frac{5 g_A^3 \Delta_3}{8 f_\pi^3} \frac{1}{\omega_k^2} \int_{\mathbf{q}} \frac{\omega_+^2 + \omega_+ \omega_- + \omega_-^2}{\omega_+^3 \omega_-^3 (\omega_+ + \omega_-)} \\
& \times \left[ \mathbf{k} \cdot \boldsymbol{\sigma}_1 (\mathbf{q} \times \mathbf{k}) \cdot \boldsymbol{\sigma}_2 (\mathbf{q} \cdot \mathbf{K}) \tau_{1z} \right. \\
& \left. - \mathbf{k} \cdot \boldsymbol{\sigma}_2 (\mathbf{q} \times \mathbf{k}) \cdot \boldsymbol{\sigma}_1 (\mathbf{q} \cdot \mathbf{K}) \tau_{2z} \right] \quad (B24)
\end{aligned}$$

while for the latter,

$$\begin{aligned}
V^{(1)}(i - \text{PNV}) = & \frac{5 g_A^3 \Delta_3}{64 f_\pi^3} \frac{1}{\omega_k^2} \left[ T_1^+ i\mathbf{k} \cdot (\boldsymbol{\sigma}_1 - \boldsymbol{\sigma}_2) \right. \\
& + T_1^- i\mathbf{k} \cdot (\boldsymbol{\sigma}_1 + \boldsymbol{\sigma}_2) \Big] \int_{\mathbf{q}} \frac{k^2 + q^2}{\omega_+ \omega_- (\omega_+ + \omega_-)} \\
& + \frac{5 g_A^3 \Delta_3}{16 f_\pi^3} \frac{1}{\omega_k^2}
\end{aligned}$$

$$\begin{aligned}
& \times \left[ (\mathbf{k} \cdot \boldsymbol{\sigma}_1 (\mathbf{k} \times \mathbf{K}) \cdot \boldsymbol{\sigma}_2 + \mathbf{k} \cdot \boldsymbol{\sigma}_2 (\mathbf{k} \times \mathbf{K}) \cdot \boldsymbol{\sigma}_1) T_1^- \right. \\
& \left. + (\mathbf{k} \cdot \boldsymbol{\sigma}_1 (\mathbf{k} \times \mathbf{K}) \cdot \boldsymbol{\sigma}_2 - \mathbf{k} \cdot \boldsymbol{\sigma}_2 (\mathbf{k} \times \mathbf{K}) \cdot \boldsymbol{\sigma}_1) T_1^+ \right] \\
& \times \int_{\mathbf{q}} \frac{1}{\omega_+ \omega_- (\omega_+ + \omega_-)} . \quad (\text{B25})
\end{aligned}$$

Also in this case we use the dimensional regularization that permits us to write the finite contribution as,

$$\begin{aligned}
\bar{V}^{(1)}(i) = & -\frac{5g_A^3 \Delta_3}{16f_\pi \Lambda_\chi^2} (T_1^- i\mathbf{k} \cdot (\boldsymbol{\sigma}_1 + \boldsymbol{\sigma}_2) \\
& + T_1^+ i\mathbf{k} \cdot (\boldsymbol{\sigma}_1 - \boldsymbol{\sigma}_2)) \\
& \times \left( \frac{25}{6} L(k) - \frac{7}{2} \frac{m_\pi^2 L(k)}{\omega_k^2} + 2 \frac{m_\pi^2 H(k)}{\omega_k^2} \right) - \frac{25g_A^3 \Delta_3}{12f_\pi \Lambda_\chi^2} \frac{1}{\omega_k^2} \\
& \times \left[ T_1^- ((\mathbf{k} \times \mathbf{K}) \cdot \boldsymbol{\sigma}_2 \mathbf{k} \cdot \boldsymbol{\sigma}_1 + (\mathbf{k} \times \mathbf{K}) \cdot \boldsymbol{\sigma}_1 \mathbf{k} \cdot \boldsymbol{\sigma}_2) \right. \\
& \left. + T_1^+ ((\mathbf{k} \times \mathbf{K}) \cdot \boldsymbol{\sigma}_2 \mathbf{k} \cdot \boldsymbol{\sigma}_1 - (\mathbf{k} \times \mathbf{K}) \cdot \boldsymbol{\sigma}_1 \mathbf{k} \cdot \boldsymbol{\sigma}_2) \right] , \quad (\text{B26})
\end{aligned}$$

while the divergent part reads,

$$\begin{aligned}
V_\infty^{(1)}(i) = & \frac{5g_A^3 \Delta_3}{16f_\pi \Lambda_\chi^2} (T_1^- i\mathbf{k} \cdot (\boldsymbol{\sigma}_1 + \boldsymbol{\sigma}_2) \\
& + T_1^+ i\mathbf{k} \cdot (\boldsymbol{\sigma}_1 - \boldsymbol{\sigma}_2)) \\
& \times \left[ \frac{m_\pi^2}{\omega_k^2} \left( \frac{151}{12} d_\epsilon - \frac{305}{18} \right) - \frac{25}{12} d_\epsilon - \frac{2}{9} \right] . \quad (\text{B27})
\end{aligned}$$

The divergences present in Eq. (B27) are reabsorbed in the  $V_{TRV}^{(\text{OPE})}$  term proportional to  $g_1$  for the part which multiply  $m_\pi^2/\omega_k^2$  and in the  $V_{TRV}^{(\text{CT})}$  term proportional to  $C_4$  for the rest. All the divergences related to the term where  $\mathbf{K}$  is present cancel out.

The N2LO contribution of panel (l) in Fig. 1 is proportional to the LECs  $c_1$ ,  $c_2$  and  $c_3$  of the PC sector and it reads,

$$\begin{aligned}
V^{(1)}(l) = & -\frac{5g_A \Delta_3 M}{2f_\pi^3} \frac{1}{\omega_k^2} \left[ T_1^+ i\mathbf{k} \cdot (\boldsymbol{\sigma}_1 - \boldsymbol{\sigma}_2) \right. \\
& \left. + T_1^- i\mathbf{k} \cdot (\boldsymbol{\sigma}_1 + \boldsymbol{\sigma}_2) \right] \left( c_1 m_\pi^2 \int_{\mathbf{q}} \frac{1}{\omega_+ \omega_- (\omega_+ + \omega_-)} \right. \\
& \left. + \frac{c_2 + c_3}{8} \int_{\mathbf{q}} \frac{1}{\omega_+ + \omega_-} - \frac{c_3}{8} \int_{\mathbf{q}} \frac{k^2 - q^2}{\omega_+ \omega_- (\omega_+ + \omega_-)} \right) . \quad (\text{B28})
\end{aligned}$$

Using dimensional regularization we obtain for the finite part,

$$\begin{aligned}
\bar{V}^{(1)}(l) = & \frac{5g_A \Delta_3 M}{2f_\pi \Lambda_\chi^2} (T_1^- i\mathbf{k} \cdot (\boldsymbol{\sigma}_1 + \boldsymbol{\sigma}_2) \\
& + T_1^+ i\mathbf{k} \cdot (\boldsymbol{\sigma}_1 - \boldsymbol{\sigma}_2)) \\
& \times \left[ 4c_1 \frac{m_\pi^2 L(k)}{\omega_k^2} - \frac{c_2}{3} \left( 2L(k) + 6 \frac{m_\pi^2}{\omega_k^2} L(k) \right) \right. \\
& \left. - \frac{c_3}{2} \left( 3L(k) + 5 \frac{m_\pi^2}{\omega_k^2} L(k) \right) \right] , \quad (\text{B29})
\end{aligned}$$

while the divergent part is given by,

$$\begin{aligned}
V_\infty^{(1)}(l) = & \frac{5g_A \Delta_3 M}{2f_\pi \Lambda_\chi^2} (T_1^- i\mathbf{k} \cdot (\boldsymbol{\sigma}_1 + \boldsymbol{\sigma}_2) \\
& + T_1^+ i\mathbf{k} \cdot (\boldsymbol{\sigma}_1 - \boldsymbol{\sigma}_2)) \left[ c_1 \frac{1}{\omega_k^2} (-2d_\epsilon + 4) \right. \\
& - \frac{c_2}{3} \left( \frac{m_\pi^2}{\omega_k^2} (5d_\epsilon - \frac{19}{3}) + (d_\epsilon - \frac{5}{3}) \right) \\
& \left. - \frac{c_3}{2} \left( \frac{m_\pi^2}{\omega_k^2} (\frac{11}{2} d_\epsilon - \frac{25}{3}) + (\frac{3}{2} d_\epsilon - \frac{2}{3}) \right) \right] . \quad (\text{B30})
\end{aligned}$$

As for the panel (i) the divergences which multiply  $m_\pi^2/\omega_k^2$  are reabsorbed in the  $V^{(\text{OPE})}$  term proportional to  $g_1$  while all the others in the  $V^{(\text{CT})}$  term proportional to  $C_4$ . At N2LO panel (l) can receive contribution also from the second order in the  $\pi NN$  and  $\pi\pi NN$  vertices but due to the isospin structure these contributions vanish.

As regarding the  $NNN$  TRV potential all the contributions come from diagrams (m) of Fig. 1. The expression we obtain at NLO is given in Eq. (33). The N2LO component would come from NLO PC  $\pi NN$  vertex or in the pion propagators. In both cases the different time-order diagrams cancel out each-other completely.

## Appendix C: The potential in configuration space

### 1. The $NN$ potential

In this subsection we present the  $NN$  potential part in the configuration space which follows directly from Eq. (31) and it reads,

$$\begin{aligned}
V_{TRV}(\mathbf{r}, \mathbf{p}) = & V^{(\text{OPE})}(\mathbf{r}) + V^{(\text{TPE})}(\mathbf{r}) + V^{(3\pi,0)}(\mathbf{r}) \\
& + V^{(3\pi,1)}(\mathbf{r}) + V^{(\text{CT})}(\mathbf{r}) + V^{(\text{RC})}(\mathbf{r}, \mathbf{p}) \\
& + V^{(3\pi, \text{RC})}(\mathbf{r}, \mathbf{p}) , \quad (\text{C1})
\end{aligned}$$

where  $\mathbf{p} = -i\nabla$  is the relative momentum operator. It is convenient to define the operators,

$$\hat{S}_\mathbf{r}^+ = (\boldsymbol{\sigma}_1 + \boldsymbol{\sigma}_2) \cdot \hat{\mathbf{r}} , \quad (\text{C2})$$

$$\hat{S}_\mathbf{r}^- = (\boldsymbol{\sigma}_1 - \boldsymbol{\sigma}_2) \cdot \hat{\mathbf{r}} , \quad (\text{C3})$$

$$\hat{S}_L^+ = -i(\boldsymbol{\sigma}_1 + \boldsymbol{\sigma}_2) \cdot (\hat{\mathbf{r}} \times \hat{\mathbf{L}}) , \quad (\text{C4})$$

$$\hat{S}_L^- = -i(\boldsymbol{\sigma}_1 - \boldsymbol{\sigma}_2) \cdot (\hat{\mathbf{r}} \times \hat{\mathbf{L}}) , \quad (\text{C5})$$

$$\hat{S}_\mathbf{r}^\times = (\boldsymbol{\sigma}_1 \times \boldsymbol{\sigma}_2) \cdot \hat{\mathbf{r}} , \quad (\text{C6})$$

$$\hat{S}_{\mathbf{r}L}^+ = \boldsymbol{\sigma}_1 \cdot \hat{\mathbf{r}} \boldsymbol{\sigma}_2 \cdot \hat{\mathbf{L}} + \boldsymbol{\sigma}_2 \cdot \hat{\mathbf{r}} \boldsymbol{\sigma}_1 \cdot \hat{\mathbf{L}} , \quad (\text{C7})$$

$$\hat{S}_{\mathbf{r}L}^- = \boldsymbol{\sigma}_1 \cdot \hat{\mathbf{r}} \boldsymbol{\sigma}_2 \cdot \hat{\mathbf{L}} - \boldsymbol{\sigma}_2 \cdot \hat{\mathbf{r}} \boldsymbol{\sigma}_1 \cdot \hat{\mathbf{L}} , \quad (\text{C8})$$

where  $\hat{\mathbf{L}} = \hat{\mathbf{r}} \times \mathbf{p}$  is the “reduced” orbital angular momentum operator. In terms of these,  $V_{TRV}(\mathbf{r}, \mathbf{p})$  can be written as

$$V^{(\text{OPE})}(\mathbf{r}) = \frac{g_A g_0^* m_\pi}{2f_\pi} T_0 \hat{S}_\mathbf{r}^- g'(r)$$

$$\begin{aligned}
& + \frac{g_A g_1 m_\pi}{4 f_\pi} \left( T_1^+ \hat{S}_r^- + T_1^- \hat{S}_r^+ \right) g'(r) \\
& + \frac{g_A g_2 m_\pi}{6 f_\pi} T_2 \hat{S}_r^- g'(r), \quad (C9)
\end{aligned}$$

$$\begin{aligned}
V^{(\text{TPE})}(\mathbf{r}) = & \frac{g_A g_0^* m_\pi^3}{f_\pi \Lambda_\chi^2} T_0 \hat{S}_r^- L'(r) \\
& + \frac{g_A^3 g_0^* m_\pi^3}{f_\pi \Lambda_\chi^2} T_0 \hat{S}_r^- (H'(r) - 3L'(r)) \\
& - \frac{g_A g_2 m_\pi^3}{3 f_\pi \Lambda_\chi^2} T_2 \hat{S}_r^- L'(r) \\
& - \frac{g_A^3 g_2 m_\pi^3}{3 f_\pi \Lambda_\chi^2} T_2 \hat{S}_r^- (H'(r) - 3L'(r)), \quad (C10)
\end{aligned}$$

$$\begin{aligned}
V^{(3\pi,0)}(\mathbf{r}) = & - \frac{5 g_A^3 \Delta_3 M m_\pi^2}{4 f_\pi \Lambda_\chi^2} \pi \\
& \times (T_1^+ \hat{S}_r^- + T_1^- \hat{S}_r^+) (A'(r) + g'(r)) \quad (C11)
\end{aligned}$$

$$\begin{aligned}
V^{(3\pi,1)}(\mathbf{r}) = & \frac{5 g_A \Delta_3 M m_\pi^3}{2 f_\pi \Lambda_\chi^2} (T_1^+ \hat{S}_r^- + T_1^- \hat{S}_r^+) \\
& \left[ 4c_1 L'_\omega(r) - \frac{c_2}{3} (2L'(r) + 6L'_\omega(r)) \right. \\
& \left. - \frac{c_3}{2} (3L'(r) + 5L'_\omega(r)) \right], \quad (C12)
\end{aligned}$$

$$\begin{aligned}
V^{(\text{CT})}(\mathbf{r}) = & \frac{m_\pi^2}{\Lambda_\chi^2 f_\pi} \left[ C_1 \hat{S}_r^- Z'(r) + C_2 T_0 \hat{S}_r^- Z'(r) \right. \\
& + \frac{C_3}{2} (T_1^+ \hat{S}_r^- - T_1^- \hat{S}_r^+) Z'(r) \\
& + \frac{C_4}{2} (T_1^+ \hat{S}_r^- + T_1^- \hat{S}_r^+) Z'(r) \\
& \left. + C_5 T_2 \hat{S}_r^- Z'(r) \right], \quad (C13)
\end{aligned}$$

$$\begin{aligned}
V^{(\text{RC})}(\mathbf{r}, \mathbf{p}) = & + \frac{g_A g_0^* m_\pi^3}{2 f_\pi M^2} T_0 \left[ \frac{\hat{S}_r^-}{4} \left( g'''(r) + 2 \frac{g''(r)}{r} - 2 \frac{g'(r)}{r^2} \right) \right. \\
& + \hat{S}_L^- \frac{g'(r)}{r^2} - \frac{g'(r)}{r^2} \hat{S}_r^- L^2 - \frac{1}{4} \left( \frac{g''(r)}{r} + \frac{g'(r)}{r^2} \right) \hat{S}_{rL}^- \\
& + \left( \hat{S}_r^- \left( g''(r) + 2 \frac{g'(r)}{r} \right) - i \frac{\hat{S}_r^\times}{2} \frac{g'(r)}{r} \right) \frac{d}{dr} \\
& + g'(r) \hat{S}_r^- \frac{d^2}{dr^2} \left. \right] \frac{1}{m_\pi^2} \\
& + \frac{g_A g_1 m_\pi^3}{4 f_\pi M^2} T_1^+ \left[ \frac{\hat{S}_r^-}{4} \left( g'''(r) + 2 \frac{g''(r)}{r} - 2 \frac{g'(r)}{r^2} \right) \right. \\
& + \hat{S}_L^- \frac{g'(r)}{r^2} - \frac{g'(r)}{r^2} \hat{S}_r^- L^2 - \frac{1}{4} \left( \frac{g''(r)}{r} + \frac{g'(r)}{r^2} \right) \hat{S}_{rL}^- \\
& + \left( \hat{S}_r^- \left( g''(r) + 2 \frac{g'(r)}{r} \right) - i \frac{\hat{S}_r^\times}{2} \frac{g'(r)}{r} \right) \frac{d}{dr} \\
& + g'(r) \hat{S}_r^- \frac{d^2}{dr^2} \left. \right] \frac{1}{m_\pi^2} \\
& + \frac{g_A g_1 m_\pi^3}{4 f_\pi M^2} T_1^- \left[ \frac{\hat{S}_r^+}{4} \left( g'''(r) + 2 \frac{g''(r)}{r} - 2 \frac{g'(r)}{r^2} \right) + \right.
\end{aligned}$$

$$\begin{aligned}
& + \hat{S}_L^+ \frac{g'(r)}{r^2} - \frac{g'(r)}{r^2} \hat{S}_r^+ L^2 - \frac{1}{4} \left( \frac{g''(r)}{r} - \frac{g'(r)}{r^2} \right) \hat{S}_{rL}^+ \\
& + \hat{S}_r^+ \left( g''(r) + 2 \frac{g'(r)}{r} \right) \frac{d}{dr} + g'(r) \hat{S}_r^+ \frac{d^2}{dr^2} \left. \right] \frac{1}{m_\pi^2} \\
& + \frac{g_A g_2 m_\pi^3}{6 f_\pi M^2} T_2 \left[ \frac{\hat{S}_r^-}{4} \left( g'''(r) + 2 \frac{g''(r)}{r} - 2 \frac{g'(r)}{r^2} \right) \right. \\
& + \hat{S}_L^- \frac{g'(r)}{r^2} - \frac{g'(r)}{r^2} \hat{S}_r^- L^2 - \frac{1}{4} \left( \frac{g''(r)}{r} + \frac{g'(r)}{r^2} \right) \hat{S}_{rL}^- \\
& + \left( \hat{S}_r^- \left( g''(r) + 2 \frac{g'(r)}{r} \right) - i \frac{\hat{S}_r^\times}{2} \frac{g'(r)}{r} \right) \frac{d}{dr} \\
& + g'(r) \hat{S}_r^- \frac{d^2}{dr^2} \left. \right] \frac{1}{m_\pi^2}, \quad (C14)
\end{aligned}$$

$$\begin{aligned}
V^{(3\pi-\text{RC})}(\mathbf{r}, \mathbf{p}) = & - \frac{5 g_A^3 \Delta_3 m_\pi^3}{16 f_\pi \Lambda_\chi^2} (T_1^+ \hat{S}_r^- + T_1^- \hat{S}_r^+) \\
& \left( \frac{25}{6} L'(r) - \frac{7}{2} L'_\omega(r) + 2H'_\omega(r) \right) \\
& + \frac{25 g_A^3 \Delta_3 m_\pi^3}{12 f_\pi \Lambda_\chi^2} \left[ T_1^+ \left( \left( \frac{g''(r)}{r} + \frac{g'(r)}{r^2} \right) \hat{S}_{rL}^- \right. \right. \\
& + 2i \hat{S}_r^\times \frac{g'(r)}{r} \frac{d}{dr} \left. \right) + T_1^- \left( \frac{g''(r)}{r} - \frac{g'(r)}{r^2} \right) \hat{S}_{rL}^+ \left. \right] \frac{1}{m_\pi^2}, \quad (C15)
\end{aligned}$$

with

$$g(r) = \int \frac{d^3 k}{(2\pi)^3} \frac{C_\Lambda(k)}{m_\pi} \frac{1}{\omega_k^2} e^{i\mathbf{k} \cdot \mathbf{r}}, \quad (C16)$$

$$L(r) = \int \frac{d^3 k}{(2\pi)^3} \frac{C_\Lambda(k)}{m_\pi^3} L(k) e^{i\mathbf{k} \cdot \mathbf{r}}, \quad (C17)$$

$$H(r) = \int \frac{d^3 k}{(2\pi)^3} \frac{C_\Lambda(k)}{m_\pi^3} H(k) e^{i\mathbf{k} \cdot \mathbf{r}}, \quad (C18)$$

$$A(r) = \int \frac{d^3 k}{(2\pi)^3} \frac{C_\Lambda(k)}{m_\pi^2} \frac{s^2 A(k)}{\omega_k^2} e^{i\mathbf{k} \cdot \mathbf{r}}, \quad (C19)$$

$$L_\omega(r) = \int \frac{d^3 k}{(2\pi)^3} \frac{C_\Lambda(k)}{m_\pi} \frac{L(k)}{\omega_k^2} e^{i\mathbf{k} \cdot \mathbf{r}}, \quad (C20)$$

$$H_\omega(r) = \int \frac{d^3 k}{(2\pi)^3} \frac{C_\Lambda(k)}{m_\pi} \frac{H(k)}{\omega_k^2} e^{i\mathbf{k} \cdot \mathbf{r}}, \quad (C21)$$

$$Z(r) = \int \frac{d^3 k}{(2\pi)^3} \frac{C_\Lambda(k)}{m_\pi^2} e^{i\mathbf{k} \cdot \mathbf{r}}. \quad (C22)$$

The functions  $g(r)$ ,  $L(r)$ ,  $H(r)$ ,  $A(r)$ ,  $L_\omega(r)$ ,  $H_\omega(r)$  and  $Z(r)$  are calculated numerically by standard quadrature techniques.

## 2. The NNN potential

In this section we present the explicit derivation of the NNN potential in configuration space. Writing explicitly the integral in Eq. (34), neglecting the deltas for simplicity, we get,



$$\begin{aligned}
V(\mathbf{x}_1, \mathbf{x}_2) = & -\frac{\Delta_3 g_A^3 M}{4f_\pi^3} T_3 \frac{1}{2} \int \frac{d^3 q}{(2\pi)^3} \frac{d^3 Q}{(2\pi)^3} e^{-i(\mathbf{q}/2) \cdot \mathbf{x}_2} e^{-i\mathbf{Q} \cdot \mathbf{x}_1} \\
& \times \frac{i(\mathbf{Q} + \mathbf{q}) \cdot \boldsymbol{\sigma}_1 i(\mathbf{Q} - \mathbf{q}) \cdot \boldsymbol{\sigma}_2 i\mathbf{Q} \cdot \boldsymbol{\sigma}_3}{\omega_+^2 \omega_-^2 \omega_Q^2}, \quad (\text{C23})
\end{aligned}$$

where  $T_3 = \boldsymbol{\tau}_1 \cdot \boldsymbol{\tau}_2 \tau_{3z} + \boldsymbol{\tau}_1 \cdot \boldsymbol{\tau}_3 \tau_{2z} + \boldsymbol{\tau}_2 \cdot \boldsymbol{\tau}_3 \tau_{1z}$ . The momenta  $\mathbf{q}$  and  $\mathbf{Q}$  in Eq. (C23) can be rewritten applying the gradient  $i\nabla$  to the exponential functions and it reads,

$$\begin{aligned}
V(\mathbf{x}_1, \mathbf{x}_2) = & \frac{\Delta_3 g_A^3 M}{4f_\pi^3} T_3 \frac{1}{2} [(\nabla_{\mathbf{x}_1} + 2\nabla_{\mathbf{x}_2}) \cdot \boldsymbol{\sigma}_1 (\nabla_{\mathbf{x}_1} - 2\nabla_{\mathbf{x}_2}) \cdot \boldsymbol{\sigma}_2 \\
& \times \nabla_{\mathbf{x}_1} \cdot \boldsymbol{\sigma}_3] \int \frac{d^3 Q}{(2\pi)^3} \frac{e^{-i\mathbf{Q} \cdot \mathbf{x}_1}}{\omega_Q^2} \int \frac{d^3 q}{(2\pi)^3} \frac{e^{-i(\mathbf{q}/2) \cdot \mathbf{x}_2}}{\omega_+^2 \omega_-^2}. \quad (\text{C24})
\end{aligned}$$

The integral in  $\mathbf{q}$  in Eq. (C24) can be solved using the Feynman tricks. The final result is

$$\begin{aligned}
V(\mathbf{x}_1, \mathbf{x}_2) = & \frac{\Delta_3 g_A^3 M}{4f_\pi^3} T_3 \frac{1}{32\pi} [(\nabla_{\mathbf{x}_1} + 2\nabla_{\mathbf{x}_2}) \cdot \boldsymbol{\sigma}_1 \\
& \times (\nabla_{\mathbf{x}_1} - 2\nabla_{\mathbf{x}_2}) \cdot \boldsymbol{\sigma}_2 \nabla_{\mathbf{x}_1} \cdot \boldsymbol{\sigma}_3] \int \frac{d^3 Q}{(2\pi)^3} \frac{e^{-i\mathbf{Q} \cdot \mathbf{x}_1}}{\omega_Q^2} \\
& \times \int_{-1}^1 dx e^{i(x/2)\mathbf{Q} \cdot \mathbf{x}_2} \frac{e^{-(L/2)x_2}}{L}, \quad (\text{C25})
\end{aligned}$$

where  $L = \sqrt{Q^2(1-x^2) + 4m_\pi^2}$ . The derivative are then evaluated obtaining five integral operators  $I_i$ ,

$$V(\mathbf{x}_1, \mathbf{x}_2) = \frac{\Delta_3 g_A^3 M}{4f_\pi^3} T_3 \sum_{i=1,5} I_i \quad (\text{C26})$$

where,

$$\begin{aligned}
I_1 = & -\frac{i}{16\pi} \int \frac{d^3 Q}{(2\pi)^3} \frac{e^{-i\mathbf{Q} \cdot \mathbf{x}_1}}{\omega_Q^2} \int_{-1}^1 dx \\
& \times e^{i(x/2)\mathbf{Q} \cdot \mathbf{x}_2} \frac{e^{-(L/2)x_2}}{x_2} (\boldsymbol{\sigma}_1 \cdot \boldsymbol{\sigma}_2) \mathbf{Q} \cdot \boldsymbol{\sigma}_3, \quad (\text{C27})
\end{aligned}$$

$$\begin{aligned}
I_2 = & +\frac{i}{32\pi} \int \frac{d^3 Q}{(2\pi)^3} \frac{e^{-i\mathbf{Q} \cdot \mathbf{x}_1}}{\omega_Q^2} \int_{-1}^1 dx (1-x^2) \\
& \times e^{i(x/2)\mathbf{Q} \cdot \mathbf{x}_2} \frac{e^{-(L/2)x_2}}{L} \mathbf{Q} \cdot \boldsymbol{\sigma}_1 \mathbf{Q} \cdot \boldsymbol{\sigma}_2 \mathbf{Q} \cdot \boldsymbol{\sigma}_3, \quad (\text{C28})
\end{aligned}$$

$$\begin{aligned}
I_3 = & -\frac{1}{32\pi} \int \frac{d^3 Q}{(2\pi)^3} \frac{e^{-i\mathbf{Q} \cdot \mathbf{x}_1}}{\omega_Q^2} \int_{-1}^1 dx (1-x) \\
& \times e^{i(x/2)\mathbf{Q} \cdot \mathbf{x}_2} e^{-(L/2)x_2} \mathbf{Q} \cdot \boldsymbol{\sigma}_1 \mathbf{x}_2 \cdot \boldsymbol{\sigma}_2 \mathbf{Q} \cdot \boldsymbol{\sigma}_3, \quad (\text{C29})
\end{aligned}$$

$$\begin{aligned}
I_4 = & +\frac{1}{32\pi} \int \frac{d^3 Q}{(2\pi)^3} \frac{e^{-i\mathbf{Q} \cdot \mathbf{x}_1}}{\omega_Q^2} \int_{-1}^1 dx (1+x) \\
& \times e^{i(x/2)\mathbf{Q} \cdot \mathbf{x}_2} e^{-(L/2)x_2} \mathbf{x}_2 \cdot \boldsymbol{\sigma}_1 \mathbf{Q} \cdot \boldsymbol{\sigma}_2 \mathbf{Q} \cdot \boldsymbol{\sigma}_3, \quad (\text{C30})
\end{aligned}$$

$$\begin{aligned}
I_5 = & +\frac{i}{32\pi} \int \frac{d^3 Q}{(2\pi)^3} \frac{e^{-i\mathbf{Q} \cdot \mathbf{x}_1}}{\omega_Q^2} \int_{-1}^1 dx \left(L + \frac{2}{x_2}\right) \\
& \times e^{i(x/2)\mathbf{Q} \cdot \mathbf{x}_2} \frac{e^{-(L/2)x_2}}{L} \mathbf{x}_2 \cdot \boldsymbol{\sigma}_1 \mathbf{x}_2 \cdot \boldsymbol{\sigma}_2 \mathbf{Q} \cdot \boldsymbol{\sigma}_3, \quad (\text{C31})
\end{aligned}$$

To be noticed that integral  $I_4 = I_3$  exchanging particle 1 and 2.

In order to divide the angular integration in  $\hat{\mathbf{Q}}$  from the radial integration in  $Q$ , the exponential functions are expanded in plane waves. Therefore the integrals  $I_i$  result,

$$I_i = \sum_{l,l'} O_i^{ll'} J_i^{ll'}, \quad (\text{C32})$$

where  $J_i$  is the integral over  $Q$  while in  $O_i$  the integral is over  $\hat{\mathbf{Q}}$ . The expressions of  $J_i$  are explicitly given below:

$$\begin{aligned}
J_1^{ll'} = & \frac{1}{8\pi} \int_{-1}^1 dx \int_0^\infty dQ \frac{Q^2}{\omega_Q^2} C_\Lambda(Q) e^{-(L/2)x_2} \\
& \times j_l\left(\frac{xQx_2}{2}\right) j_{l'}(Qx_1) \frac{Q}{x_2}, \quad (\text{C33})
\end{aligned}$$

$$\begin{aligned}
J_2^{ll'} = & \frac{1}{16\pi} \int_{-1}^1 dx \int_0^\infty dQ \frac{Q^2}{\omega_Q^2} C_\Lambda(Q) e^{-(L/2)x_2} \\
& \times j_l\left(\frac{xQx_2}{2}\right) j_{l'}(Qx_1) \frac{Q^3}{L} (1-x^2), \quad (\text{C34})
\end{aligned}$$

$$\begin{aligned}
J_3^{ll'} = & \frac{1}{16\pi} \int_{-1}^1 dx \int_0^\infty dQ \frac{Q^2}{\omega_Q^2} C_\Lambda(Q) e^{-(L/2)x_2} \\
& \times j_l\left(\frac{xQx_2}{2}\right) j_{l'}(Qx_1) Q^2 (1-x), \quad (\text{C35})
\end{aligned}$$

$$\begin{aligned}
J_4^{ll'} = & \frac{1}{16\pi} \int_{-1}^1 dx \int_0^\infty dQ \frac{Q^2}{\omega_Q^2} C_\Lambda(Q) e^{-(L/2)x_2} \\
& \times j_l\left(\frac{xQx_2}{2}\right) j_{l'}(Qx_1) Q^2 (1+x), \quad (\text{C36})
\end{aligned}$$

$$\begin{aligned}
J_5^{ll'} = & \frac{1}{16\pi} \int_{-1}^1 dx \int_0^\infty dQ \frac{Q^2}{\omega_Q^2} C_\Lambda(Q) e^{-(L/2)x_2} \\
& \times j_l\left(\frac{xQx_2}{2}\right) j_{l'}(Qx_1) Q \left(L - \frac{2}{x_2}\right), \quad (\text{C37})
\end{aligned}$$

where  $j_l(x)$  are spherical Bessel functions and we include a regularization function  $C_\Lambda(Q)$  which is defined in Eq. (35). The functions  $J_i$  depend only on the modules of  $\mathbf{x}_1$  and  $\mathbf{x}_2$  and they are evaluated numerically by standard quadrature techniques.

For the  $O_i$  integrals we get,

$$\begin{aligned}
O_1^{ll'} = & (-i)i^{l'}(-i)^l \hat{l} \hat{l}' \int d\hat{\mathbf{Q}} \left[ Y_{l'}(\hat{\mathbf{Q}}) Y_l(\hat{\mathbf{x}}_1) \right]_0 \\
& \times \left[ Y_l(\hat{\mathbf{Q}}) Y_{l'}(\hat{\mathbf{x}}_2) \right]_0 \boldsymbol{\sigma}_1 \cdot \boldsymbol{\sigma}_2 \hat{\mathbf{Q}} \cdot \boldsymbol{\sigma}_3, \quad (\text{C38})
\end{aligned}$$

$$\begin{aligned}
O_2^{ll'} = & (+i)i^{l'}(-i)^l \hat{l} \hat{l}' \int d\hat{\mathbf{Q}} \left[ Y_{l'}(\hat{\mathbf{Q}}) Y_l(\hat{\mathbf{x}}_1) \right]_0 \\
& \times \left[ Y_l(\hat{\mathbf{Q}}) Y_{l'}(\hat{\mathbf{x}}_2) \right]_0 \hat{\mathbf{Q}} \cdot \boldsymbol{\sigma}_1 \hat{\mathbf{Q}} \cdot \boldsymbol{\sigma}_2 \hat{\mathbf{Q}} \cdot \boldsymbol{\sigma}_3, \quad (\text{C39})
\end{aligned}$$

$$O_3^{ll'} = -i^{l'}(-i)^l \hat{l} \hat{l}' \int d\hat{Q} \left[ Y_{l'}(\hat{Q}) Y_l(\hat{x}_1) \right]_0 \\ \times \left[ Y_l(\hat{Q}) Y_l(\hat{x}_2) \right]_0 \hat{Q} \cdot \sigma_1 \hat{x}_2 \cdot \sigma_2 \hat{Q} \cdot \sigma_3, \quad (C40)$$

$$O_4^{ll'} = +i^{l'}(-i)^l \hat{l} \hat{l}' \int d\hat{Q} \left[ Y_{l'}(\hat{Q}) Y_l(\hat{x}_1) \right]_0 \\ \times \left[ Y_l(\hat{Q}) Y_l(\hat{x}_2) \right]_0 \hat{x}_2 \cdot \sigma_1 \hat{Q} \cdot \sigma_2 \hat{Q} \cdot \sigma_3, \quad (C41)$$

$$O_5^{ll'} = (+i)^{l'}(-i)^l \hat{l} \hat{l}' \int d\hat{Q} \left[ Y_{l'}(\hat{Q}) Y_l(\hat{x}_1) \right]_0 \\ \times \left[ Y_l(\hat{Q}) Y_l(\hat{x}_2) \right]_0 \hat{x}_2 \cdot \sigma_1 \hat{x}_2 \cdot \sigma_2 \hat{Q} \cdot \sigma_3, \quad (C42)$$

which depend only to the angular part of the spatial coordinates  $\mathbf{x}_1$  and  $\mathbf{x}_2$ . The matrix element of the  $O_i$  operators between HH functions can easily expressed in terms of products of 9-j, 6-j and 3-j Wigner symbols.

#### Appendix D: Details of the calculation and convergence of the $a_\Delta(3N)$ coefficient

In order to compute the even-parity  $|\psi_+^A\rangle$  and odd-parity  $|\psi_-^A\rangle$  component of the wave function we need to solve the following eigenvalue problem,

$$\begin{pmatrix} V_{PC}^{++} & V_{TRV}^{+-} \\ V_{TRV}^{-+} & V_{PC}^{--} \end{pmatrix} \begin{pmatrix} |\psi_+^A\rangle \\ |\psi_-^A\rangle \end{pmatrix} = E \begin{pmatrix} |\psi_+^A\rangle \\ |\psi_-^A\rangle \end{pmatrix}. \quad (D1)$$

Using the fact that  $\|V_{TRV}\| \ll \|V_{PC}\|$  we can rewrite the eigenvalue problem of Eq. (D1) as,

$$\begin{cases} V_{PC}^{++} |\psi_+^A\rangle = E |\psi_+^A\rangle \\ |\psi_-^A\rangle = -(V_{PC}^{--} - E)^{-1} V_{TRV}^{-+} |\psi_+^A\rangle \end{cases}, \quad (D2)$$

where the first equation is the standard eigenvalue problem, while with the second we can compute the odd component of the wave function. This approach from the numerical point of view results more stable than solving directly Eq. (D1) and permits to study the odd component of the wave function without solving every time the eigenvalue problem.

Let us study now the convergence pattern of the  $a_\Delta(3N)$  coefficient, defined in Eq. (46), in term of the

grandangular momentum  $K$  of the HH basis (for more details, see Ref. [58, 59]). Increasing  $K$  is equivalent of enlarging the expansion basis. To be definite, in this appendix, we have considered the  $^3\text{H}$  case and used the N4LO/N2LO-500 PC interaction.

Let us denote with  $K^+$  ( $K^-$ ) the maximum value of the grandangular momentum of the HH functions used to describe the even (odd) part of the wave function  $|\psi_+^A\rangle$  ( $|\psi_-^A\rangle$ ). We have computed the even part of the wave function up to complete convergence ( $K^+ = 50$ ) obtaining a binding energy  $B(^3\text{H}) = 8.476$  MeV using the first formula in Eq. (D2). For solving the second equation of Eq. (D2) we have performed different calculations varying  $K^-$  and we have reported the corresponding results for  $a_\Delta(3N)$  in Table VIII. As can be seen by inspecting the table, the pattern of convergence is very smooth. A safe convergence at the third digit is reached for  $K^- \sim 21$ , which was the value also selected for performing the final calculations. On the other hand, the value of  $a_\Delta(3N)$  is not much sensitive to  $K^+$ , in particular when  $K^+ > 20$ . Therefore, the value of the coefficient  $a_\Delta(3N)$  appears to be well under control in our calculation.

$K^-$	$a_\Delta(3N)$
5	-0.1728
9	-0.1842
13	-0.1879
17	-0.1892
21	-0.1897

TABLE VIII. Convergence pattern of the  $^3\text{H}$   $a_\Delta(3N)$  coefficient as function of  $K^-$ , the maximum grandangular momentum of the HH functions used for constructing the odd-parity component of the  $^3\text{H}$  wave function. For the even-parity we have used  $K^+ = 50$ , a value sufficient to reach full convergence of the even-parity component of the wave function. The reported calculations are performed using N4LO/N2LO-500 PC interaction.

- 
- |  |  |
|--|--|
| <p>[1] A.D. Sakharov, Pisma Zh. Eksp. Teor. Fiz. <b>5</b>, 32 (1967).<br/> [2] A.G. Cohen, D.B. Kaplan, and A.E. Nelson, Ann. Rev. Nucl. Part. Sci. <b>43</b>, 27 (1993).<br/> [3] G. 't Hooft, Phys. Rev. Lett. <b>37</b>, 8 (1976).<br/> [4] M. Pospelov, A. Ritz, Annals Phys. <b>318</b>, 119 (2005).<br/> [5] A. Czarnecki and B. Krause, Phys. Rev. Lett. <b>78</b>, 4339 (1997).<br/> [6] T. Mannel and N. Uraltsev, Phys. Rev. D <b>85</b>, 096002 (2012).<br/> [7] T. Mannel and N. Uraltsev, JHEP <b>03</b>, 064 (2013).</p> | <p>[8] C.A. Baker <i>et al.</i>, Phys. Rev. Lett. <b>97</b> 131801 (2006).<br/> [9] W.C. Griffith, M.D. Swallows, T.H. Loftus, M.V. Romalis, B.R. Heckel, and E.N. Fortson, Phys. Rev. Lett. <b>102</b>, 101601 (2009).<br/> [10] V.F. Dmitriev and R.A. Senkov Phys. Rev. Lett. <b>91</b>, 212303 (2003).<br/> [11] J. Baron <i>et al.</i> Science <b>343</b> (6168), 269 (2014).<br/> [12] Y.F. Orlov, W.M. Morse and Y.K. Semertzidis, Phys. Rev. Lett. <b>96</b>, 214802 (2006).<br/> [13] Y.K. Semertzidis, Proceedings of the DPF 2011 Confer-</p> |
|--|--|

- ence (2011).
- [14] A. Lehrach, B. Lorentz, W. Morse, N. Nikolaev and F. Rathmann, arXiv:1201.5773 (2013)
  - [15] J. Pretz, *Hyperfine Interact.* **214** (1-3), 111 (2013).
  - [16] F. Rathmann, A. Saleev and N.N. Nikolaev, *J. Phys. Conf. Ser.* **447**, 012011 (2013).
  - [17] P.K. Kabir, *Phys. Rev. D* **25**, 2013 (1982).
  - [18] L. Stodolsky, *Nucl. Phys. B* **197**, 213 (1982).
  - [19] C.-P. Liu and R.G.E. Timmermans, *Phys. Rev. C* **70**, 055501 (2004).
  - [20] C.-P. Liu, R.G.E. Timmermans, *Phys. Lett. B* **634**, 488 (2006).
  - [21] J. D. Bowman and V. Gudkov, *Phys. Rev. C* **90**, 065503 (2014).
  - [22] Y.-H. Song, R. Lazauskas, and V. Gudkov, *Phys. Rev. C* **83**, 065503 (2011).
  - [23] Yu. N. Uzikov and A. A. Temerbayev, *Int. Journal of Modern Physics: Conf. Series* **40**, 1660080 (2016); Yu. N. Uzikov and J. Haidenbauer, *Phys. Rev. C* **94**, 035501 (2016).
  - [24] V. Gudkov and H. M. Shimizu, *Phys. Rev. C* **97**, 065502 (2018).
  - [25] P. Fadeev and V. V. Flambaum, arXiv:1903.08937.
  - [26] D.R. Entem, N. Kaiser, R. Machleidt, Y. Nosyk, *Phys. Rev. C* **91**, 014002 (2015).
  - [27] E. Epelbaum, H. Krebs and U.-G. Meissner, *Phys. Rev. Lett.* **115**, 122301 (2015).
  - [28] T.-S. Park, D.-P. Min, and M. Rho, *Nucl. Phys. A* **596**, 515 (1996); Y.-H. Song, R. Lazauskas, and T.-S. Park, *Phys. Rev. C* **79**, 064002 (2009).
  - [29] T.-S. Park *et al.*, *Phys. Rev. C* **67**, 055206 (2003).
  - [30] S. Kölling, E. Epelbaum, H. Krebs, and U.-G. Meissner, *Phys. Rev. C* **80**, 045502 (2009).
  - [31] S. Pastore, L. Girlanda, R. Schiavilla, M. Viviani, and R.B. Wiringa *Phys. Rev. C* **80**, 034004 (2009).
  - [32] S. Kölling, E. Epelbaum, H. Krebs, and U.-G. Meissner, *Phys. Rev. C* **84**, 054008 (2011).
  - [33] S. Pastore, L. Girlanda, R. Schiavilla, and M. Viviani, *Phys. Rev. C* **84**, 024001 (2011).
  - [34] M. Piarulli *et al.*, *Phys. Rev. C* **87**, 014006 (2013).
  - [35] S. Weinberg, *Phys. Rev. Lett.* **17**, 616 (1966); *Phys. Rev.* **166**, 1568 (1968); *Physica A* **96**, 327 (1979).
  - [36] C. Callan, S. Coleman, J. Wess, and B. Zumino, *Phys. Rev.* **177**, 2247 (1969).
  - [37] E. Mereghetti, W.H. Hockings and U. van Kolck, *Annals Phys.* **325**, 2363 (2010).
  - [38] J. Bsaisou, Ulf-G. Meissner, A. Nogga and A. Wirzba, *Annals Phys.* **359**, 317 (2015).
  - [39] B. Grzadkowski, M. Iskrzynski, M. Misiak, and J. Rosiek, *JHEP* **1010**, 085 (2010).
  - [40] J. de Vries, E. Mereghetti, R.G.E. Timmermans and U. van Kolck, *Annals Phys.* **338**, 50 (2013).
  - [41] W. Dekens and J. de Vries, *JHEP* **1305**, 149 (2013).
  - [42] J. de Vries, E. Mereghetti, R.G.E. Timmermans, and U. van Kolck, *Phys. Rev. Lett.* **107**, 091804 (2011).
  - [43] W. Dekens *et al.*, *JHEP* **07**, 069 (2014).
  - [44] C. M. Maekawa, E. Mereghetti, J. de Vries, and U. van Kolck, *Nucl. Phys. A* **872**, 117 (2011).
  - [45] J. Bsaisou, C. Hanhart, S. Liebig, U.-G. Meissner, A. Nogga, and A. Wirzba, *Eur. Phys. J. A* **49**, 31 (2013).
  - [46] J. de Vries, *et al.*, *Phys. Rev. C* **84**, 065501 (2011)
  - [47] J. Bsaisou, J. de Vries, C. Hanhart, S. Liebig, Ulf-G. Meissner, D. Minossi, A. Nogga, and A. Wirzba, *JHEP* **03**, 104 (2015), erratum *JHEP* **05**, 083 (2015).
  - [48] I. Stetcu, C.-P. Liu, J.L. Friar, A.C. Hayes, and P. Navratil, *Phys. Lett. B* **665**, 168 (2008).
  - [49] N. Yamanaka and E. Hiyama, *Phys. Rev. C* **91**, 054005 (2015)
  - [50] Y.-H. Song, R. Lazauskas, and V. Gudkov *Phys. Rev. C* **87**, 015501 (2013)
  - [51] M. Viviani, *et al.*, *Phys. Rev. C* **89**, 064004 (2014).
  - [52] N. Fettes, *et al.*, *Ann. Phys.* **283**, 273 (2000).
  - [53] E. Epelbaum, H. W. Hammer, and U.-G. Meissner, *Rev. Mod. Phys.* **81**, 1773 (2009).
  - [54] R. Machleidt and D. R. Entem, *Phys. Rep.* **503**, 1 (2011).
  - [55] L. Girlanda, S. Pastore, R. Schiavilla, and M. Viviani, *Phys. Rev. C* **81**, 034005 (2010).
  - [56] L.E. Marcucci, F. Sammarruca, M. Viviani, R. Machleidt, arXiv:1809.01849.
  - [57] E. Epelbaum, W. Glöckle, and U.-G. Meissner, *Nucl. Phys. A* **747**, 362 (2005)
  - [58] A. Kievsky, S. Rosati, M. Viviani, L.E. Marcucci, and L. Girlanda, *J. Phys. G: Nucl. Part. Phys.* **35**, 063101 (2008).
  - [59] L.E. Marcucci, A. Kievsky, L. Girlanda, S. Rosati, and M. Viviani, *Phys. Rev. C* **80**, 034003 (2009).